Open data from the first and second observing runs of Advanced LIGO and Advanced Virgo

R. Abbott,[1] T. D. Abbott,[2] S. Abraham,[3] F. Acernese,[4,5]
K. Ackley,[6] C. Adams,[7] R. X. Adhikari,[1] V. B. Adya,[8]
C. Affeldt,[9,10] M. Agathos,[11,12] K. Agatsuma,[13] N. Aggarwal,[14]
O. D. Aguiar,[15] A. Aich,[16] L. Aiello,[17,18] A. Ain,[3] P. Ajith,[19]
G. Allen,[20] A. Allocca,[21] P. A. Altin,[8] A. Amato,[22] S. Anand,[1]
A. Ananyeva,[1] S. B. Anderson,[1] W. G. Anderson,[23]
S. V. Angelova,[24] S. Ansoldi,[25,26] S. Antier,[27] S. Appert,[1] K. Arai,[1]
M. C. Araya,[1] J. S. Areeda,[28] M. Arène,[27] N. Arnaud,[29,30]
S. M. Aronson,[31] K. G. Arun,[32] S. Ascenzi,[17,33] G. Ashton,[6]
S. M. Aston,[7] P. Astone,[34] F. Aubin,[35] P. Aufmuth,[10]
K. AultONeal,[36] C. Austin,[2] V. Avendano,[37] S. Babak,[27]
P. Bacon,[27] F. Badaracco,[17,18] M. K. M. Bader,[38] S. Bae,[39]
A. M. Baer,[40] J. Baird,[27] F. Baldaccini,[41,42] G. Ballardin,[30]
S. W. Ballmer,[43] A. Bals,[36] A. Balsamo,[40] G. Baltus,[44]
S. Banagiri,[45] D. Bankar,[3] R. S. Bankar,[3] J. C. Barayoga,[1]
C. Barbieri,[46,47] B. C. Barish,[1] D. Barker,[48] K. Barkett,[49]
P. Barneo,[50] F. Barone,[51,5] B. Barr,[52] L. Barsotti,[53] M. Barsuglia,[27]
D. Barta,[54] J. Bartlett,[48] I. Bartos,[31] R. Bassiri,[55] A. Basti,[56,21]
M. Bawaj,[57,42] J. C. Bayley,[52] M. Bazzan,[58,59] B. Bécsy,[60]
M. Bejger,[61] I. Belahcene,[29] A. S. Bell,[52] D. Beniwal,[62]
M. G. Benjamin,[36] J. D. Bentley,[13] F. Bergamin,[9] B. K. Berger,[55]
G. Bergmann,[9,10] S. Bernuzzi,[11] C. P. L. Berry,[14] D. Bersanetti,[63]
A. Bertolini,[38] J. Betzwieser,[7] R. Bhandare,[64] A. V. Bhandari,[3]
J. Bidler,[28] E. Biggs,[23] I. A. Bilenko,[65] G. Billingsley,[1] R. Birney,[66]
O. Birnholtz,[67,68] S. Biscans,[1,53] M. Bischi,[69,70] S. Biscoveanu,[53]
A. Bisht,[10] G. Bissenbayeva,[16] M. Bitossi,[30,21] M. A. Bizouard,[71]
J. K. Blackburn,[1] J. Blackman,[49] C. D. Blair,[7] D. G. Blair,[72]
R. M. Blair,[48] F. Bobba,[73,74] N. Bode,[9,10] M. Boer,[71] Y. Boetzel,[75]
G. Bogaert,[71] F. Bondu,[76] E. Bonilla,[55] R. Bonnand,[35]
P. Booker,[9,10] B. A. Boom,[38] R. Bork,[1] V. Boschi,[21] S. Bose,[3]
V. Bossilkov,[72] J. Bosveld,[72] Y. Bouffanais,[58,59] A. Bozzi,[30]
C. Bradaschia,[21] P. R. Brady,[23] A. Bramley,[7] M. Branchesi,[17,18]

J. E. Brau,[77] M. Breschi,[11] T. Briant,[78] J. H. Briggs,[52]
F. Brighenti,[69,70] A. Brillet,[71] M. Brinkmann,[9,10] P. Brockill,[23]
A. F. Brooks,[1] J. Brooks,[30] D. D. Brown,[62] S. Brunett,[1]
G. Bruno,[79] R. Bruntz,[40] A. Buikema,[53] T. Bulik,[80]
H. J. Bulten,[81,38] A. Buonanno,[82,83] D. Buskulic,[35] R. L. Byer,[55]
M. Cabero,[9,10] L. Cadonati,[84] G. Cagnoli,[85] C. Cahillane,[1]
J. Calderón Bustillo,[6] J. D. Callaghan,[52] T. A. Callister,[1]
E. Calloni,[86,5] J. B. Camp,[87] M. Canepa,[88,63] K. C. Cannon,[89]
H. Cao,[62] J. Cao,[90] G. Carapella,[73,74] F. Carbognani,[30] S. Caride,[91]
M. F. Carney,[14] G. Carullo,[56,21] J. Casanueva Diaz,[21]
C. Casentini,[92,33] J. Castañeda,[50] S. Caudill,[38] M. Cavaglià,[93]
F. Cavalier,[29] R. Cavalieri,[30] G. Cella,[21] P. Cerdá-Durán,[94]
E. Cesarini,[95,33] O. Chaibi,[71] K. Chakravarti,[3] C. Chan,[89]
M. Chan,[52] S. Chao,[96] P. Charlton,[97] E. A. Chase,[14]
E. Chassande-Mottin,[27] D. Chatterjee,[23] M. Chaturvedi,[64]
H. Y. Chen,[100] X. Chen,[72] Y. Chen,[49] H.-P. Cheng,[31]
C. K. Cheong,[101] H. Y. Chia,[31] F. Chiadini,[102,74] R. Chierici,[103]
A. Chincarini,[63] A. Chiummo,[30] G. Cho,[104] H. S. Cho,[105]
M. Cho,[83] N. Christensen,[71] Q. Chu,[72] S. Chua,[78] K. W. Chung,[101]
S. Chung,[72] G. Ciani,[58,59] P. Ciecielag,[61] M. Cieślar,[61]
A. A. Ciobanu,[62] R. Ciolfi,[106,59] F. Cipriano,[71] A. Cirone,[88,63]
F. Clara,[48] J. A. Clark,[84] P. Clearwater,[107] S. Clesse,[79] F. Cleva,[71]
E. Coccia,[17,18] P.-F. Cohadon,[78] D. Cohen,[29] M. Colleoni,[108]
C. G. Collette,[109] C. Collins,[13] M. Colpi,[46,47] M. Constancio Jr.,[15]
L. Conti,[59] S. J. Cooper,[13] P. Corban,[7] T. R. Corbitt,[2]
I. Cordero-Carrión,[110] S. Corezzi,[41,42] K. R. Corley,[111]
N. Cornish,[60] D. Corre,[29] A. Corsi,[91] S. Cortese,[30] C. A. Costa,[15]
R. Cotesta,[82] M. W. Coughlin,[1] S. B. Coughlin,[112,14]
J.-P. Coulon,[71] S. T. Countryman,[111] P. Couvares,[1] P. B. Covas,[108]
D. M. Coward,[72] M. J. Cowart,[7] D. C. Coyne,[1] R. Coyne,[113]
J. D. E. Creighton,[23] T. D. Creighton,[16] J. Cripe,[2] M. Croquette,[78]
S. G. Crowder,[114] J.-R. Cudell,[44] T. J. Cullen,[2] A. Cumming,[52]
R. Cummings,[52] L. Cunningham,[52] E. Cuoco,[30] M. Curylo,[80]
T. Dal Canton,[82] G. Dálya,[115] A. Dana,[55]
L. M. Daneshgaran-Bajastani,[116] B. D'Angelo,[88,63]
S. L. Danilishin,[9,10] S. D'Antonio,[33] K. Danzmann,[10,9]
C. Darsow-Fromm,[117] A. Dasgupta,[118] L. E. H. Datrier,[52]
V. Dattilo,[30] I. Dave,[64] M. Davier,[29] G. S. Davies,[119] D. Davis,[43]
E. J. Daw,[120] D. DeBra,[55] M. Deenadayalan,[3] J. Degallaix,[22]

M. De Laurentis,[86,5] S. Deléglise,[78] M. Delfavero,[67] N. De Lillo,[52]
W. Del Pozzo,[56,21] L. M. DeMarchi,[14] V. D'Emilio,[112] N. Demos,[53]
T. Dent,[119] R. De Pietri,[121,122] R. De Rosa,[86,5] C. De Rossi,[30]
R. DeSalvo,[123] O. de Varona,[9,10] S. Dhurandhar,[3] M. C. Díaz,[16]
M. Diaz-Ortiz Jr.,[31] T. Dietrich,[38] L. Di Fiore,[5] C. Di Fronzo,[13]
C. Di Giorgio,[73,74] F. Di Giovanni,[94] M. Di Giovanni,[124,125]
T. Di Girolamo,[86,5] A. Di Lieto,[56,21] B. Ding,[109] S. Di Pace,[126,34]
I. Di Palma,[126,34] F. Di Renzo,[56,21] A. K. Divakarla,[31]
A. Dmitriev,[13] Z. Doctor,[100] F. Donovan,[53] K. L. Dooley,[112]
S. Doravari,[3] I. Dorrington,[112] T. P. Downes,[23] M. Drago,[17,18]
J. C. Driggers,[48] Z. Du,[90] J.-G. Ducoin,[29] P. Dupej,[52]
O. Durante,[73,74] D. D'Urso,[127,128] S. E. Dwyer,[48] P. J. Easter,[6]
G. Eddolls,[52] B. Edelman,[77] T. B. Edo,[120] O. Edy,[129] A. Effler,[7]
P. Ehrens,[1] J. Eichholz,[8] S. S. Eikenberry,[31] M. Eisenmann,[35]
R. A. Eisenstein,[53] A. Ejlli,[112] L. Errico,[86,5] R. C. Essick,[100]
H. Estelles,[108] D. Estevez,[35] Z. B. Etienne,[130] T. Etzel,[1]
M. Evans,[53] T. M. Evans,[7] B. E. Ewing,[131] V. Fafone,[92,33,17]
S. Fairhurst,[112] X. Fan,[90] S. Farinon,[63] B. Farr,[77] W. M. Farr,[98,99]
E. J. Fauchon-Jones,[112] M. Favata,[37] M. Fays,[120] M. Fazio,[132]
J. Feicht,[1] M. M. Fejer,[55] F. Feng,[27] E. Fenyvesi,[54,133]
D. L. Ferguson,[84] A. Fernandez-Galiana,[53] I. Ferrante,[56,21]
E. C. Ferreira,[15] T. A. Ferreira,[15] F. Fidecaro,[56,21] I. Fiori,[30]
D. Fiorucci,[17,18] M. Fishbach,[100] R. P. Fisher,[40] R. Fittipaldi,[134,74]
M. Fitz-Axen,[45] V. Fiumara,[135,74] R. Flaminio,[35,136] E. Floden,[45]
E. Flynn,[28] H. Fong,[89] J. A. Font,[94,137] P. W. F. Forsyth,[8]
J.-D. Fournier,[71] S. Frasca,[126,34] F. Frasconi,[21] Z. Frei,[115]
A. Freise,[13] R. Frey,[77] V. Frey,[29] P. Fritschel,[53] V. V. Frolov,[7]
G. Fronzè,[138] P. Fulda,[31] M. Fyffe,[7] H. A. Gabbard,[52]
B. U. Gadre,[82] S. M. Gaebel,[13] J. R. Gair,[82] S. Galaudage,[6]
D. Ganapathy,[53] S. G. Gaonkar,[3] C. García-Quirós,[108]
F. Garufi,[86,5] B. Gateley,[48] S. Gaudio,[36] V. Gayathri,[139]
G. Gemme,[63] E. Genin,[30] A. Gennai,[21] D. George,[20] J. George,[64]
L. Gergely,[140] S. Ghonge,[84] Abhirup Ghosh,[82]
Archisman Ghosh,[141,142,143,38] S. Ghosh,[23] B. Giacomazzo,[124,125]
J. A. Giaime,[2,7] K. D. Giardina,[7] D. R. Gibson,[66] C. Gier,[24]
K. Gill,[111] J. Glanzer,[2] J. Gniesmer,[117] P. Godwin,[131] E. Goetz,[2,93]
R. Goetz,[31] N. Gohlke,[9,10] B. Goncharov,[6] G. González,[2]
A. Gopakumar,[144] S. E. Gossan,[1] M. Gosselin,[30,56,21] R. Gouaty,[35]
B. Grace,[8] A. Grado,[145,5] M. Granata,[22] A. Grant,[52] S. Gras,[53]

P. Grassia,[1] C. Gray,[48] R. Gray,[52] G. Greco,[69,70] A. C. Green,[31]
R. Green,[112] E. M. Gretarsson,[36] H. L. Griggs,[84] G. Grignani,[41,42]
A. Grimaldi,[124,125] S. J. Grimm,[17,18] H. Grote,[112] S. Grunewald,[82]
P. Gruning,[29] G. M. Guidi,[69,70] A. R. Guimaraes,[2] G. Guixé,[50]
H. K. Gulati,[118] Y. Guo,[38] A. Gupta,[131] Anchal Gupta,[1]
P. Gupta,[38] E. K. Gustafson,[1] R. Gustafson,[146] L. Haegel,[108]
O. Halim,[18,17] E. D. Hall,[53] E. Z. Hamilton,[112] G. Hammond,[52]
M. Haney,[75] M. M. Hanke,[9,10] J. Hanks,[48] C. Hanna,[131]
M. D. Hannam,[112] O. A. Hannuksela,[101] T. J. Hansen,[36]
J. Hanson,[7] T. Harder,[71] T. Hardwick,[2] K. Haris,[19] J. Harms,[17,18]
G. M. Harry,[147] I. W. Harry,[129] R. K. Hasskew,[7] C.-J. Haster,[53]
K. Haughian,[52] F. J. Hayes,[52] J. Healy,[67] A. Heidmann,[78]
M. C. Heintze,[7] J. Heinze,[9,10] H. Heitmann,[71] F. Hellman,[148]
P. Hello,[29] G. Hemming,[30] M. Hendry,[52] I. S. Heng,[52] E. Hennes,[38]
J. Hennig,[9,10] M. Heurs,[9,10] S. Hild,[149,52] T. Hinderer,[143,38,141]
S. Y. Hoback,[28,147] S. Hochheim,[9,10] E. Hofgard,[55] D. Hofman,[22]
A. M. Holgado,[20] N. A. Holland,[8] K. Holt,[7] D. E. Holz,[100]
P. Hopkins,[112] C. Horst,[23] J. Hough,[52] E. J. Howell,[72] C. G. Hoy,[112]
Y. Huang,[53] M. T. Hübner,[6] E. A. Huerta,[20] D. Huet,[29]
B. Hughey,[36] V. Hui,[35] S. Husa,[108] S. H. Huttner,[52] R. Huxford,[131]
T. Huynh-Dinh,[7] B. Idzkowski,[80] A. Iess,[92,33] H. Inchauspe,[31]
C. Ingram,[62] G. Intini,[126,34] J.-M. Isac,[78] M. Isi,[53] B. R. Iyer,[19]
T. Jacqmin,[78] S. J. Jadhav,[150] S. P. Jadhav,[3] A. L. James,[112]
K. Jani,[84] N. N. Janthalur,[150] P. Jaranowski,[151] D. Jariwala,[31]
R. Jaume,[108] A. C. Jenkins,[152] J. Jiang,[31] G. R. Johns,[40]
A. W. Jones,[13] D. I. Jones,[153] J. D. Jones,[48] P. Jones,[13] R. Jones,[52]
R. J. G. Jonker,[38] L. Ju,[72] J. Junker,[9,10] C. V. Kalaghatgi,[112]
V. Kalogera,[14] B. Kamai,[1] S. Kandhasamy,[3] G. Kang,[39]
J. B. Kanner,[1] S. J. Kapadia,[19] S. Karki,[77] R. Kashyap,[19]
M. Kasprzack,[1] W. Kastaun,[9,10] S. Katsanevas,[30]
E. Katsavounidis,[53] W. Katzman,[7] S. Kaufer,[10] K. Kawabe,[48]
F. Kéfélian,[71] D. Keitel,[129] A. Keivani,[111] R. Kennedy,[120]
J. S. Key,[154] S. Khadka,[55] F. Y. Khalili,[65] I. Khan,[17,33] S. Khan,[9,10]
Z. A. Khan,[90] E. A. Khazanov,[155] N. Khetan,[17,18] M. Khursheed,[64]
N. Kijbunchoo,[8] Chunglee Kim,[156] G. J. Kim,[84] J. C. Kim,[157]
K. Kim,[101] W. Kim,[62] W. S. Kim,[158] Y.-M. Kim,[159] C. Kimball,[14]
P. J. King,[48] M. Kinley-Hanlon,[52] R. Kirchhoff,[9,10] J. S. Kissel,[48]
L. Kleybolte,[117] S. Klimenko,[31] T. D. Knowles,[130] P. Koch,[9,10]
S. M. Koehlenbeck,[9,10] G. Koekoek,[38,149] S. Koley,[38]

V. Kondrashov,[1] A. Kontos,[160] N. Koper,[9,10] M. Korobko,[117]
W. Z. Korth,[1] M. Kovalam,[72] D. B. Kozak,[1] V. Kringel,[9,10]
N. V. Krishnendu,[32] A. Królak,[161,162] N. Krupinski,[23] G. Kuehn,[9,10]
A. Kumar,[150] P. Kumar,[163] Rahul Kumar,[48] Rakesh Kumar,[118]
S. Kumar,[19] L. Kuo,[96] A. Kutynia,[161] B. D. Lackey,[82] D. Laghi,[56,21]
E. Lalande,[164] T. L. Lam,[101] A. Lamberts,[71,165] M. Landry,[48]
B. B. Lane,[53] R. N. Lang,[166] J. Lange,[67] B. Lantz,[55] R. K. Lanza,[53]
I. La Rosa,[35] A. Lartaux-Vollard,[29] P. D. Lasky,[6] M. Laxen,[7]
A. Lazzarini,[1] C. Lazzaro,[59] P. Leaci,[126,34] S. Leavey,[9,10]
Y. K. Lecoeuche,[48] C. H. Lee,[105] H. M. Lee,[167] H. W. Lee,[157]
J. Lee,[104] K. Lee,[55] J. Lehmann,[9,10] N. Leroy,[29] N. Letendre,[35]
Y. Levin,[6] A. K. Y. Li,[101] J. Li,[90] K. li,[101] T. G. F. Li,[101] X. Li,[49]
F. Linde,[168,38] S. D. Linker,[116] J. N. Linley,[52] T. B. Littenberg,[169]
J. Liu,[9,10] X. Liu,[23] M. Llorens-Monteagudo,[94] R. K. L. Lo,[1]
A. Lockwood,[170] L. T. London,[53] A. Longo,[171,172] M. Lorenzini,[17,18]
V. Loriette,[173] M. Lormand,[7] G. Losurdo,[21] J. D. Lough,[9,10]
C. O. Lousto,[67] G. Lovelace,[28] H. Lück,[10,9] D. Lumaca,[92,33]
A. P. Lundgren,[129] Y. Ma,[49] R. Macas,[112] S. Macfoy,[24]
M. MacInnis,[53] D. M. Macleod,[112] I. A. O. MacMillan,[147]
A. Macquet,[71] I. Magaña Hernandez,[23] F. Magaña-Sandoval,[31]
R. M. Magee,[131] E. Majorana,[34] I. Maksimovic,[173] A. Malik,[64]
N. Man,[71] V. Mandic,[45] V. Mangano,[52,126,34] G. L. Mansell,[48,53]
M. Manske,[23] M. Mantovani,[30] M. Mapelli,[58,59]
F. Marchesoni,[57,42,174] F. Marion,[35] S. Márka,[111] Z. Márka,[111]
C. Markakis,[12] A. S. Markosyan,[55] A. Markowitz,[1] E. Maros,[1]
A. Marquina,[110] S. Marsat,[27] F. Martelli,[69,70] I. W. Martin,[52]
R. M. Martin,[37] V. Martinez,[85] D. V. Martynov,[13]
H. Masalehdan,[117] K. Mason,[53] E. Massera,[120] A. Masserot,[35]
T. J. Massinger,[53] M. Masso-Reid,[52] S. Mastrogiovanni,[27]
A. Matas,[82] F. Matichard,[1,53] N. Mavalvala,[53] E. Maynard,[2]
J. J. McCann,[72] R. McCarthy,[48] D. E. McClelland,[8]
S. McCormick,[7] L. McCuller,[53] S. C. McGuire,[175] C. McIsaac,[129]
J. McIver,[1] D. J. McManus,[8] T. McRae,[8] S. T. McWilliams,[130]
D. Meacher,[23] G. D. Meadors,[6] M. Mehmet,[9,10] A. K. Mehta,[19]
E. Mejuto Villa,[123,74] A. Melatos,[107] G. Mendell,[48] R. A. Mercer,[23]
L. Mereni,[22] K. Merfeld,[77] E. L. Merilh,[48] J. D. Merritt,[77]
M. Merzougui,[71] S. Meshkov,[1] C. Messenger,[52] C. Messick,[176]
R. Metzdorff,[78] P. M. Meyers,[107] F. Meylahn,[9,10] A. Mhaske,[3]
A. Miani,[124,125] H. Miao,[13] I. Michaloliakos,[31] C. Michel,[22]

H. Middleton,[107] L. Milano,[86,5] A. L. Miller,[31,126,34]
M. Millhouse,[107] J. C. Mills,[112] E. Milotti,[177,26]
M. C. Milovich-Goff,[116] O. Minazzoli,[71,178] Y. Minenkov,[33]
A. Mishkin,[31] C. Mishra,[179] T. Mistry,[120] S. Mitra,[3]
V. P. Mitrofanov,[65] G. Mitselmakher,[31] R. Mittleman,[53] G. Mo,[53]
K. Mogushi,[93] S. R. P. Mohapatra,[53] S. R. Mohite,[23]
M. Molina-Ruiz,[148] M. Mondin,[116] M. Montani,[69,70] C. J. Moore,[13]
D. Moraru,[48] F. Morawski,[61] G. Moreno,[48] S. Morisaki,[89]
B. Mours,[180] C. M. Mow-Lowry,[13] S. Mozzon,[129] F. Muciaccia,[126,34]
Arunava Mukherjee,[52] D. Mukherjee,[131] S. Mukherjee,[16]
Subroto Mukherjee,[118] N. Mukund,[9,10] A. Mullavey,[7] J. Munch,[62]
E. A. Muñiz,[43] P. G. Murray,[52] A. Nagar,[95,138,181]
I. Nardecchia,[92,33] L. Naticchioni,[126,34] R. K. Nayak,[182]
B. F. Neil,[72] J. Neilson,[123,74] G. Nelemans,[183,38] T. J. N. Nelson,[7]
M. Nery,[9,10] A. Neunzert,[146] K. Y. Ng,[53] S. Ng,[62] C. Nguyen,[27]
P. Nguyen,[77] D. Nichols,[143,38] S. A. Nichols,[2] S. Nissanke,[143,38]
F. Nocera,[30] M. Noh,[53] C. North,[112] D. Nothard,[184]
L. K. Nuttall,[129] J. Oberling,[48] B. D. O'Brien,[31] G. Oganesyan,[17,18]
G. H. Ogin,[185] J. J. Oh,[158] S. H. Oh,[158] F. Ohme,[9,10] H. Ohta,[89]
M. A. Okada,[15] M. Oliver,[108] C. Olivetto,[30] P. Oppermann,[9,10]
Richard J. Oram,[7] B. O'Reilly,[7] R. G. Ormiston,[45] L. F. Ortega,[31]
R. O'Shaughnessy,[67] S. Ossokine,[82] C. Osthelder,[1] D. J. Ottaway,[62]
H. Overmier,[7] B. J. Owen,[91] A. E. Pace,[131] G. Pagano,[56,21]
M. A. Page,[72] G. Pagliaroli,[17,18] A. Pai,[139] S. A. Pai,[64]
J. R. Palamos,[77] O. Palashov,[155] C. Palomba,[34] H. Pan,[96]
P. K. Panda,[150] P. T. H. Pang,[38] C. Pankow,[14] F. Pannarale,[126,34]
B. C. Pant,[64] F. Paoletti,[21] A. Paoli,[30] A. Parida,[3] W. Parker,[7,175]
D. Pascucci,[52,38] A. Pasqualetti,[30] R. Passaquieti,[56,21]
D. Passuello,[21] B. Patricelli,[56,21] E. Payne,[6] B. L. Pearlstone,[52]
T. C. Pechsiri,[31] A. J. Pedersen,[43] M. Pedraza,[1] A. Pele,[7]
S. Penn,[186] A. Perego,[124,125] C. J. Perez,[48] C. Périgois,[35]
A. Perreca,[124,125] S. Perriès,[103] J. Petermann,[117] H. P. Pfeiffer,[82]
M. Phelps,[9,10] K. S. Phukon,[3,168,38] O. J. Piccinni,[126,34]
M. Pichot,[71] M. Piendibene,[56,21] F. Piergiovanni,[69,70]
V. Pierro,[123,74] G. Pillant,[30] L. Pinard,[22] I. M. Pinto,[123,74,95]
K. Piotrzkowski,[79] M. Pirello,[48] M. Pitkin,[187] W. Plastino,[171,172]
R. Poggiani,[56,21] D. Y. T. Pong,[101] S. Ponrathnam,[3] P. Popolizio,[30]
E. K. Porter,[27] J. Powell,[188] A. K. Prajapati,[118] K. Prasai,[55]
R. Prasanna,[150] G. Pratten,[13] T. Prestegard,[23] M. Principe,[123,95,74]

G. A. Prodi,[124,125] L. Prokhorov,[13] M. Punturo,[42] P. Puppo,[34]
M. Pürrer,[82] H. Qi,[112] V. Quetschke,[16] P. J. Quinonez,[36]
F. J. Raab,[48] G. Raaijmakers,[143,38] H. Radkins,[48] N. Radulesco,[71]
P. Raffai,[115] H. Rafferty,[189] S. Raja,[64] C. Rajan,[64]
B. Rajbhandari,[91] M. Rakhmanov,[16] K. E. Ramirez,[16]
A. Ramos-Buades,[108] Javed Rana,[3] K. Rao,[14] P. Rapagnani,[126,34]
V. Raymond,[112] M. Razzano,[56,21] J. Read,[28] T. Regimbau,[35]
L. Rei,[63] S. Reid,[24] D. H. Reitze,[1,31] P. Rettegno,[138,190]
F. Ricci,[126,34] C. J. Richardson,[36] J. W. Richardson,[1]
P. M. Ricker,[20] G. Riemenschneider,[190,138] K. Riles,[146] M. Rizzo,[14]
N. A. Robertson,[1,52] F. Robinet,[29] A. Rocchi,[33]
R. D. Rodriguez-Soto,[36] L. Rolland,[35] J. G. Rollins,[1] V. J. Roma,[77]
M. Romanelli,[76] R. Romano,[4,5] C. L. Romel,[48]
I. M. Romero-Shaw,[6] J. H. Romie,[7] C. A. Rose,[23] D. Rose,[28]
K. Rose,[184] D. Rosińska,[80] S. G. Rosofsky,[20] M. P. Ross,[170]
S. Rowan,[52] S. J. Rowlinson,[13] P. K. Roy,[16] Santosh Roy,[3]
Soumen Roy,[191] P. Ruggi,[30] G. Rutins,[66] K. Ryan,[48] S. Sachdev,[131]
T. Sadecki,[48] M. Sakellariadou,[152] O. S. Salafia,[192,46,47] L. Salconi,[30]
M. Saleem,[32] A. Samajdar,[38] E. J. Sanchez,[1] L. E. Sanchez,[1]
N. Sanchis-Gual,[193] J. R. Sanders,[194] K. A. Santiago,[37] E. Santos,[71]
N. Sarin,[6] B. Sassolas,[22] B. S. Sathyaprakash,[131,112] O. Sauter,[35]
R. L. Savage,[48] V. Savant,[3] D. Sawant,[139] S. Sayah,[22] D. Schaetzl,[1]
P. Schale,[77] M. Scheel,[49] J. Scheuer,[14] P. Schmidt,[13]
R. Schnabel,[117] R. M. S. Schofield,[77] A. Schönbeck,[117]
E. Schreiber,[9,10] B. W. Schulte,[9,10] B. F. Schutz,[112] O. Schwarm,[185]
E. Schwartz,[7] J. Scott,[52] S. M. Scott,[8] E. Seidel,[20] D. Sellers,[7]
A. S. Sengupta,[191] N. Sennett,[82] D. Sentenac,[30] V. Sequino,[63]
A. Sergeev,[155] Y. Setyawati,[9,10] D. A. Shaddock,[8] T. Shaffer,[48]
M. S. Shahriar,[14] A. Sharma,[17,18] P. Sharma,[64] P. Shawhan,[83]
H. Shen,[20] M. Shikauchi,[89] R. Shink,[164] D. H. Shoemaker,[53]
D. M. Shoemaker,[84] K. Shukla,[148] S. ShyamSundar,[64] K. Siellez,[84]
M. Sieniawska,[61] D. Sigg,[48] L. P. Singer,[87] D. Singh,[131] N. Singh,[80]
A. Singha,[52] A. Singhal,[17,34] A. M. Sintes,[108] V. Sipala,[127,128]
V. Skliris,[112] B. J. J. Slagmolen,[8] T. J. Slaven-Blair,[72]
J. Smetana,[13] J. R. Smith,[28] R. J. E. Smith,[6] S. Somala,[195]
E. J. Son,[158] S. Soni,[2] B. Sorazu,[52] V. Sordini,[103] F. Sorrentino,[63]
T. Souradeep,[3] E. Sowell,[91] A. P. Spencer,[52] M. Spera,[58,59]
A. K. Srivastava,[118] V. Srivastava,[43] K. Staats,[14] C. Stachie,[71]
M. Standke,[9,10] D. A. Steer,[27] M. Steinke,[9,10] J. Steinlechner,[117,52]

S. Steinlechner,[117] D. Steinmeyer,[9,10] D. Stocks,[55] D. J. Stops,[13]
M. Stover,[184] K. A. Strain,[52] G. Stratta,[196,70] A. Strunk,[48]
R. Sturani,[197] A. L. Stuver,[198] S. Sudhagar,[3] V. Sudhir,[53]
T. Z. Summerscales,[199] L. Sun,[1] S. Sunil,[118] A. Sur,[61] J. Suresh,[89]
P. J. Sutton,[112] B. L. Swinkels,[38] M. J. Szczepańczyk,[31]
M. Tacca,[38] S. C. Tait,[52] C. Talbot,[6] A. J. Tanasijczuk,[79]
D. B. Tanner,[31] D. Tao,[1] M. Tápai,[140] A. Tapia,[28]
E. N. Tapia San Martin,[38] J. D. Tasson,[200] R. Taylor,[1]
R. Tenorio,[108] L. Terkowski,[117] M. P. Thirugnanasambandam,[3]
M. Thomas,[7] P. Thomas,[48] J. E. Thompson,[112] S. R. Thondapu,[64]
K. A. Thorne,[7] E. Thrane,[6] C. L. Tinsman,[6] T. R. Saravanan,[3]
Shubhanshu Tiwari,[75,124,125] S. Tiwari,[144] V. Tiwari,[112]
K. Toland,[52] M. Tonelli,[56,21] Z. Tornasi,[52] A. Torres-Forné,[82]
C. I. Torrie,[1] I. Tosta e Melo,[127,128] D. Töyrä,[8] E. A. Trail,[2]
F. Travasso,[57,42] G. Traylor,[7] M. C. Tringali,[80] A. Tripathee,[146]
A. Trovato,[27] R. J. Trudeau,[1] K. W. Tsang,[38] M. Tse,[53] R. Tso,[49]
L. Tsukada,[89] D. Tsuna,[89] T. Tsutsui,[89] M. Turconi,[71] A. S. Ubhi,[13]
K. Ueno,[89] D. Ugolini,[189] C. S. Unnikrishnan,[144] A. L. Urban,[2]
S. A. Usman,[100] A. C. Utina,[52] H. Vahlbruch,[10] G. Vajente,[1]
G. Valdes,[2] M. Valentini,[124,125] M. Vallisneri,[204,205] N. van Bakel,[38]
M. van Beuzekom,[38] J. F. J. van den Brand,[81,149,38]
C. Van Den Broeck,[38,201] D. C. Vander-Hyde,[43]
L. van der Schaaf,[38] J. V. Van Heijningen,[72] A. A. van Veggel,[52]
M. Vardaro,[58,59] V. Varma,[49] S. Vass,[1] M. Vasúth,[54] A. Vecchio,[13]
G. Vedovato,[59] J. Veitch,[52] P. J. Veitch,[62] K. Venkateswara,[170]
G. Venugopalan,[1] D. Verkindt,[35] D. Veske,[111] F. Vetrano,[69,70]
A. Viceré,[69,70] A. D. Viets,[202] S. Vinciguerra,[13] D. J. Vine,[66]
J.-Y. Vinet,[71] S. Vitale,[53] Francisco Hernandez Vivanco,[6] T. Vo,[43]
H. Vocca,[41,42] C. Vorvick,[48] S. P. Vyatchanin,[65] A. R. Wade,[8]
L. E. Wade,[184] M. Wade,[184] R. Walet,[38] M. Walker,[28]
G. S. Wallace,[24] L. Wallace,[1] S. Walsh,[23] J. Z. Wang,[146] S. Wang,[20]
W. H. Wang,[16] Y. F. Wang,[101] R. L. Ward,[8] Z. A. Warden,[36]
J. Warner,[48] M. Was,[35] J. Watchi,[109] B. Weaver,[48] L.-W. Wei,[9,10]
M. Weinert,[9,10] A. J. Weinstein,[1] R. Weiss,[53] F. Wellmann,[9,10]
L. Wen,[72] P. Weßels,[9,10] J. W. Westhouse,[36] K. Wette,[8]
J. T. Whelan,[67] B. F. Whiting,[31] C. Whittle,[53] D. M. Wilken,[9,10]
D. Williams,[52] R. D. Williams,[203] J. L. Willis,[1] B. Willke,[10,9]
W. Winkler,[9,10] C. C. Wipf,[1] H. Wittel,[9,10] G. Woan,[52]
J. Woehler,[9,10] J. K. Wofford,[67] C. Wong,[101] J. L. Wright,[52]

D. S. Wu,[9,10] D. M. Wysocki,[67] L. Xiao,[1] H. Yamamoto,[1]
L. Yang,[132] Y. Yang,[31] Z. Yang,[45] M. J. Yap,[8] M. Yazback,[31]
D. W. Yeeles,[112] Hang Yu,[53] Haocun Yu,[53] S. H. R. Yuen,[101]
A. K. Zadrożny,[16] A. Zadrożny,[161] M. Zanolin,[36] T. Zelenova,[30]
J.-P. Zendri,[59] M. Zevin,[14] J. Zhang,[72] L. Zhang,[1] T. Zhang,[52]
C. Zhao,[72] G. Zhao,[109] M. Zhou,[14] Z. Zhou,[14] X. J. Zhu,[6]
A. B. Zimmerman,[176] M. E. Zucker,[53,1] and J. Zweizig[1]

(The LIGO Scientific Collaboration and the Virgo Collaboration)

December 30, 2019

[1]LIGO, California Institute of Technology, Pasadena, CA 91125, USA

[2]Louisiana State University, Baton Rouge, LA 70803, USA

[3]Inter-University Centre for Astronomy and Astrophysics, Pune 411007, India

[4]Dipartimento di Farmacia, Università di Salerno, I-84084 Fisciano, Salerno, Italy

[5]INFN, Sezione di Napoli, Complesso Universitario di Monte S.Angelo, I-80126 Napoli, Italy

[6]OzGrav, School of Physics & Astronomy, Monash University, Clayton 3800, Victoria, Australia

[7]LIGO Livingston Observatory, Livingston, LA 70754, USA

[8]OzGrav, Australian National University, Canberra, Australian Capital Territory 0200, Australia

[9]Max Planck Institute for Gravitational Physics (Albert Einstein Institute), D-30167 Hannover, Germany

[10]Leibniz Universität Hannover, D-30167 Hannover, Germany

[11]Theoretisch-Physikalisches Institut, Friedrich-Schiller-Universität Jena, D-07743 Jena, Germany

[12]University of Cambridge, Cambridge CB2 1TN, UK

[13]University of Birmingham, Birmingham B15 2TT, UK

[14]Center for Interdisciplinary Exploration & Research in Astrophysics (CIERA), Northwestern University, Evanston, IL 60208, USA

[15]Instituto Nacional de Pesquisas Espaciais, 12227-010 São José dos Campos, São Paulo, Brazil

[16]The University of Texas Rio Grande Valley, Brownsville, TX 78520, USA

[17]Gran Sasso Science Institute (GSSI), I-67100 L'Aquila, Italy

[18]INFN, Laboratori Nazionali del Gran Sasso, I-67100 Assergi, Italy

[19]International Centre for Theoretical Sciences, Tata Institute of Fundamental Research, Bengaluru 560089, India

[20]NCSA, University of Illinois at Urbana-Champaign, Urbana, IL 61801, USA

[21]INFN, Sezione di Pisa, I-56127 Pisa, Italy
[22]Laboratoire des Matériaux Avancés (LMA), IP2I - UMR 5822, CNRS, Université de Lyon, F-69622 Villeurbanne, France
[23]University of Wisconsin-Milwaukee, Milwaukee, WI 53201, USA
[24]SUPA, University of Strathclyde, Glasgow G1 1XQ, UK
[25]Dipartimento di Matematica e Informatica, Università di Udine, I-33100 Udine, Italy
[26]INFN, Sezione di Trieste, I-34127 Trieste, Italy
[27]APC, AstroParticule et Cosmologie, Université Paris Diderot, CNRS/IN2P3, CEA/Irfu, Observatoire de Paris, Sorbonne Paris Cité, F-75205 Paris Cedex 13, France
[28]California State University Fullerton, Fullerton, CA 92831, USA
[29]LAL, Univ. Paris-Sud, CNRS/IN2P3, Université Paris-Saclay, F-91898 Orsay, France
[30]European Gravitational Observatory (EGO), I-56021 Cascina, Pisa, Italy
[31]University of Florida, Gainesville, FL 32611, USA
[32]Chennai Mathematical Institute, Chennai 603103, India
[33]INFN, Sezione di Roma Tor Vergata, I-00133 Roma, Italy
[34]INFN, Sezione di Roma, I-00185 Roma, Italy
[35]Laboratoire d'Annecy de Physique des Particules (LAPP), Univ. Grenoble Alpes, Université Savoie Mont Blanc, CNRS/IN2P3, F-74941 Annecy, France
[36]Embry-Riddle Aeronautical University, Prescott, AZ 86301, USA
[37]Montclair State University, Montclair, NJ 07043, USA
[38]Nikhef, Science Park 105, 1098 XG Amsterdam, The Netherlands
[39]Korea Institute of Science and Technology Information, Daejeon 34141, South Korea
[40]Christopher Newport University, Newport News, VA 23606, USA
[41]Università di Perugia, I-06123 Perugia, Italy
[42]INFN, Sezione di Perugia, I-06123 Perugia, Italy
[43]Syracuse University, Syracuse, NY 13244, USA
[44]Université de Liège, B-4000 Liège, Belgium
[45]University of Minnesota, Minneapolis, MN 55455, USA
[46]Università degli Studi di Milano-Bicocca, I-20126 Milano, Italy
[47]INFN, Sezione di Milano-Bicocca, I-20126 Milano, Italy
[48]LIGO Hanford Observatory, Richland, WA 99352, USA
[49]Caltech CaRT, Pasadena, CA 91125, USA
[50]Departament de Física Quàntica i Astrofísica, Institut de Ciències del Cosmos (ICCUB), Universitat de Barcelona (IEEC-UB), E-08028 Barcelona, Spain
[51]Dipartimento di Medicina, Chirurgia e Odontoiatria "Scuola Medica Salernitana," Università di Salerno, I-84081 Baronissi, Salerno, Italy
[52]SUPA, University of Glasgow, Glasgow G12 8QQ, UK
[53]LIGO, Massachusetts Institute of Technology, Cambridge, MA 02139, USA
[54]Wigner RCP, RMKI, H-1121 Budapest, Konkoly Thege Miklós út 29-33, Hungary
[55]Stanford University, Stanford, CA 94305, USA
[56]Università di Pisa, I-56127 Pisa, Italy

[57]Università di Camerino, Dipartimento di Fisica, I-62032 Camerino, Italy
[58]Università di Padova, Dipartimento di Fisica e Astronomia, I-35131 Padova, Italy
[59]INFN, Sezione di Padova, I-35131 Padova, Italy
[60]Montana State University, Bozeman, MT 59717, USA
[61]Nicolaus Copernicus Astronomical Center, Polish Academy of Sciences, 00-716, Warsaw, Poland
[62]OzGrav, University of Adelaide, Adelaide, South Australia 5005, Australia
[63]INFN, Sezione di Genova, I-16146 Genova, Italy
[64]RRCAT, Indore, Madhya Pradesh 452013, India
[65]Faculty of Physics, Lomonosov Moscow State University, Moscow 119991, Russia
[66]SUPA, University of the West of Scotland, Paisley PA1 2BE, UK
[67]Rochester Institute of Technology, Rochester, NY 14623, USA
[68]Bar-Ilan University, Ramat Gan 5290002, Israel
[69]Università degli Studi di Urbino "Carlo Bo," I-61029 Urbino, Italy
[70]INFN, Sezione di Firenze, I-50019 Sesto Fiorentino, Firenze, Italy
[71]Artemis, Université Côte d'Azur, Observatoire Côte d'Azur, CNRS, CS 34229, F-06304 Nice Cedex 4, France
[72]OzGrav, University of Western Australia, Crawley, Western Australia 6009, Australia
[73]Dipartimento di Fisica "E.R. Caianiello," Università di Salerno, I-84084 Fisciano, Salerno, Italy
[74]INFN, Sezione di Napoli, Gruppo Collegato di Salerno, Complesso Universitario di Monte S. Angelo, I-80126 Napoli, Italy
[75]Physik-Institut, University of Zurich, Winterthurerstrasse 190, 8057 Zurich, Switzerland
[76]Univ Rennes, CNRS, Institut FOTON - UMR6082, F-3500 Rennes, France
[77]University of Oregon, Eugene, OR 97403, USA
[78]Laboratoire Kastler Brossel, Sorbonne Université, CNRS, ENS-Université PSL, Collège de France, F-75005 Paris, France
[79]Université catholique de Louvain, B-1348 Louvain-la-Neuve, Belgium
[80]Astronomical Observatory Warsaw University, 00-478 Warsaw, Poland
[81]VU University Amsterdam, 1081 HV Amsterdam, The Netherlands
[82]Max Planck Institute for Gravitational Physics (Albert Einstein Institute), D-14476 Potsdam-Golm, Germany
[83]University of Maryland, College Park, MD 20742, USA
[84]School of Physics, Georgia Institute of Technology, Atlanta, GA 30332, USA
[85]Université de Lyon, Université Claude Bernard Lyon 1, CNRS, Institut Lumière Matière, F-69622 Villeurbanne, France
[86]Università di Napoli "Federico II," Complesso Universitario di Monte S.Angelo, I-80126 Napoli, Italy
[87]NASA Goddard Space Flight Center, Greenbelt, MD 20771, USA
[88]Dipartimento di Fisica, Università degli Studi di Genova, I-16146 Genova, Italy

[89]RESCEU, University of Tokyo, Tokyo, 113-0033, Japan.
[90]Tsinghua University, Beijing 100084, China
[91]Texas Tech University, Lubbock, TX 79409, USA
[92]Università di Roma Tor Vergata, I-00133 Roma, Italy
[93]Missouri University of Science and Technology, Rolla, MO 65409, USA
[94]Departamento de Astronomía y Astrofísica, Universitat de València, E-46100 Burjassot, València, Spain
[95]Museo Storico della Fisica e Centro Studi e Ricerche "Enrico Fermi," I-00184 Roma, Italy
[96]National Tsing Hua University, Hsinchu City, 30013 Taiwan, Republic of China
[97]Charles Sturt University, Wagga Wagga, New South Wales 2678, Australia
[98]Physics and Astronomy Department, Stony Brook University, Stony Brook, NY 11794, USA
[99]Center for Computational Astrophysics, Flatiron Institute, 162 5th Ave, New York, NY 10010, USA
[100]University of Chicago, Chicago, IL 60637, USA
[101]The Chinese University of Hong Kong, Shatin, NT, Hong Kong
[102]Dipartimento di Ingegneria Industriale (DIIN), Università di Salerno, I-84084 Fisciano, Salerno, Italy
[103]Institut de Physique des 2 Infinis de Lyon (IP2I) - UMR 5822, Université de Lyon, Université Claude Bernard, CNRS, F-69622 Villeurbanne, France
[104]Seoul National University, Seoul 08826, South Korea
[105]Pusan National University, Busan 46241, South Korea
[106]INAF, Osservatorio Astronomico di Padova, I-35122 Padova, Italy
[107]OzGrav, University of Melbourne, Parkville, Victoria 3010, Australia
[108]Universitat de les Illes Balears, IAC3—IEEC, E-07122 Palma de Mallorca, Spain
[109]Université Libre de Bruxelles, Brussels 1050, Belgium
[110]Departamento de Matemáticas, Universitat de València, E-46100 Burjassot, València, Spain
[111]Columbia University, New York, NY 10027, USA
[112]Cardiff University, Cardiff CF24 3AA, UK
[113]University of Rhode Island, Kingston, RI 02881, USA
[114]Bellevue College, Bellevue, WA 98007, USA
[115]MTA-ELTE Astrophysics Research Group, Institute of Physics, Eötvös University, Budapest 1117, Hungary
[116]California State University, Los Angeles, 5151 State University Dr, Los Angeles, CA 90032, USA
[117]Universität Hamburg, D-22761 Hamburg, Germany
[118]Institute for Plasma Research, Bhat, Gandhinagar 382428, India
[119]IGFAE, Campus Sur, Universidade de Santiago de Compostela, 15782 Spain
[120]The University of Sheffield, Sheffield S10 2TN, UK
[121]Dipartimento di Scienze Matematiche, Fisiche e Informatiche, Università di Parma, I-43124 Parma, Italy

[122]INFN, Sezione di Milano Bicocca, Gruppo Collegato di Parma, I-43124 Parma, Italy
[123]Dipartimento di Ingegneria, Università del Sannio, I-82100 Benevento, Italy
[124]Università di Trento, Dipartimento di Fisica, I-38123 Povo, Trento, Italy
[125]INFN, Trento Institute for Fundamental Physics and Applications, I-38123 Povo, Trento, Italy
[126]Università di Roma "La Sapienza," I-00185 Roma, Italy
[127]Università degli Studi di Sassari, I-07100 Sassari, Italy
[128]INFN, Laboratori Nazionali del Sud, I-95125 Catania, Italy
[129]University of Portsmouth, Portsmouth, PO1 3FX, UK
[130]West Virginia University, Morgantown, WV 26506, USA
[131]The Pennsylvania State University, University Park, PA 16802, USA
[132]Colorado State University, Fort Collins, CO 80523, USA
[133]Institute for Nuclear Research (Atomki), Hungarian Academy of Sciences, Bem tér 18/c, H-4026 Debrecen, Hungary
[134]CNR-SPIN, c/o Università di Salerno, I-84084 Fisciano, Salerno, Italy
[135]Scuola di Ingegneria, Università della Basilicata, I-85100 Potenza, Italy
[136]National Astronomical Observatory of Japan, 2-21-1 Osawa, Mitaka, Tokyo 181-8588, Japan
[137]Observatori Astronòmic, Universitat de València, E-46980 Paterna, València, Spain
[138]INFN Sezione di Torino, I-10125 Torino, Italy
[139]Indian Institute of Technology Bombay, Powai, Mumbai 400 076, India
[140]University of Szeged, Dóm tér 9, Szeged 6720, Hungary
[141]Delta Institute for Theoretical Physics, Science Park 904, 1090 GL Amsterdam, The Netherlands
[142]Lorentz Institute, Leiden University, PO Box 9506, Leiden 2300 RA, The Netherlands
[143]GRAPPA, Anton Pannekoek Institute for Astronomy and Institute for High-Energy Physics, University of Amsterdam, Science Park 904, 1098 XH Amsterdam, The Netherlands
[144]Tata Institute of Fundamental Research, Mumbai 400005, India
[145]INAF, Osservatorio Astronomico di Capodimonte, I-80131 Napoli, Italy
[146]University of Michigan, Ann Arbor, MI 48109, USA
[147]American University, Washington, D.C. 20016, USA
[148]University of California, Berkeley, CA 94720, USA
[149]Maastricht University, P.O. Box 616, 6200 MD Maastricht, The Netherlands
[150]Directorate of Construction, Services & Estate Management, Mumbai 400094 India
[151]University of Białystok, 15-424 Białystok, Poland
[152]King's College London, University of London, London WC2R 2LS, UK
[153]University of Southampton, Southampton SO17 1BJ, UK
[154]University of Washington Bothell, Bothell, WA 98011, USA
[155]Institute of Applied Physics, Nizhny Novgorod, 603950, Russia

[156]Ewha Womans University, Seoul 03760, South Korea
[157]Inje University Gimhae, South Gyeongsang 50834, South Korea
[158]National Institute for Mathematical Sciences, Daejeon 34047, South Korea
[159]Ulsan National Institute of Science and Technology, Ulsan 44919, South Korea
[160]Bard College, 30 Campus Rd, Annandale-On-Hudson, NY 12504, USA
[161]NCBJ, 05-400 Świerk-Otwock, Poland
[162]Institute of Mathematics, Polish Academy of Sciences, 00656 Warsaw, Poland
[163]Cornell University, Ithaca, NY 14850, USA
[164]Université de Montréal/Polytechnique, Montreal, Quebec H3T 1J4, Canada
[165]Lagrange, Université Côte d'Azur, Observatoire Côte d'Azur, CNRS, CS 34229, F-06304 Nice Cedex 4, France
[166]Hillsdale College, Hillsdale, MI 49242, USA
[167]Korea Astronomy and Space Science Institute, Daejeon 34055, South Korea
[168]Institute for High-Energy Physics, University of Amsterdam, Science Park 904, 1098 XH Amsterdam, The Netherlands
[169]NASA Marshall Space Flight Center, Huntsville, AL 35811, USA
[170]University of Washington, Seattle, WA 98195, USA
[171]Dipartimento di Matematica e Fisica, Università degli Studi Roma Tre, I-00146 Roma, Italy
[172]INFN, Sezione di Roma Tre, I-00146 Roma, Italy
[173]ESPCI, CNRS, F-75005 Paris, France
[174]Center for Phononics and Thermal Energy Science, School of Physics Science and Engineering, Tongji University, 200092 Shanghai, People's Republic of China
[175]Southern University and A&M College, Baton Rouge, LA 70813, USA
[176]Department of Physics, University of Texas, Austin, TX 78712, USA
[177]Dipartimento di Fisica, Università di Trieste, I-34127 Trieste, Italy
[178]Centre Scientifique de Monaco, 8 quai Antoine Ier, MC-98000, Monaco
[179]Indian Institute of Technology Madras, Chennai 600036, India
[180]Université de Strasbourg, CNRS, IPHC UMR 7178, F-67000 Strasbourg, France
[181]Institut des Hautes Etudes Scientifiques, F-91440 Bures-sur-Yvette, France
[182]IISER-Kolkata, Mohanpur, West Bengal 741252, India
[183]Department of Astrophysics/IMAPP, Radboud University Nijmegen, P.O. Box 9010, 6500 GL Nijmegen, The Netherlands
[184]Kenyon College, Gambier, OH 43022, USA
[185]Whitman College, 345 Boyer Avenue, Walla Walla, WA 99362 USA
[186]Hobart and William Smith Colleges, Geneva, NY 14456, USA
[187]Department of Physics, Lancaster University, Lancaster, LA1 4YB, UK
[188]OzGrav, Swinburne University of Technology, Hawthorn VIC 3122, Australia
[189]Trinity University, San Antonio, TX 78212, USA

[190]Dipartimento di Fisica, Università degli Studi di Torino, I-10125 Torino, Italy
[191]Indian Institute of Technology, Gandhinagar Ahmedabad Gujarat 382424, India
[192]INAF, Osservatorio Astronomico di Brera sede di Merate, I-23807 Merate, Lecco, Italy
[193]Centro de Astrofísica e Gravitação (CENTRA), Departamento de Física, Instituto Superior Técnico, Universidade de Lisboa, 1049-001 Lisboa, Portugal
[194]Marquette University, 11420 W. Clybourn St., Milwaukee, WI 53233, USA
[195]Indian Institute of Technology Hyderabad, Sangareddy, Khandi, Telangana 502285, India
[196]INAF, Osservatorio di Astrofisica e Scienza dello Spazio, I-40129 Bologna, Italy
[197]International Institute of Physics, Universidade Federal do Rio Grande do Norte, Natal RN 59078-970, Brazil
[198]Villanova University, 800 Lancaster Ave, Villanova, PA 19085, USA
[199]Andrews University, Berrien Springs, MI 49104, USA
[200]Carleton College, Northfield, MN 55057, USA
[201]Department of Physics, Utrecht University, 3584CC Utrecht, The Netherlands
[202]Concordia University Wisconsin, 2800 N Lake Shore Dr, Mequon, WI 53097, USA
[203]Institute for Astronomy, University of Edinburgh, Royal Observatory, Blackford Hill, EH9 3HJ, UK
[204]Jet Propulsion Laboratory, California Institute of Technology, 4800 Oak Grove Drive, Pasadena, CA 91109, USA
[205]Theoretical AstroPhysics Including Relativity (TAPIR), MC 350-17, California Institute of Technology, Pasadena, California 91125, USA

Abstract

Advanced LIGO and Advanced Virgo are actively monitoring the sky and collecting gravitational-wave strain data with sufficient sensitivity to detect signals routinely. In this paper we describe the data recorded by these instruments during their first and second observing runs. The main data products are the gravitational-wave strain arrays, released as time series sampled at 16384 Hz. The datasets that include this strain measurement can be freely accessed through the Gravitational Wave Open Science Center at `http://gw-openscience.org`, together with data-quality information essential for the analysis of LIGO and Virgo data, documentation, tutorials, and supporting software.

Background and summary

Gravitational waves (GWs) are transverse waves in the spacetime metric that travel at the speed of light, which, to leading order, are generated by temporal variations of the mass quadrupole [1], as in the orbital motion of a binary system of compact stars. GWs were predicted in 1916 by Albert Einstein after the final formulation of the field equations of general relativity [2, 3]. They were first observed directly in 2015 [4] by the Laser Interferometer Gravitational-Wave Observatory (LIGO) [5] during its first observing run (O1), which took place from September 12, 2015 to January 19, 2016.

After an upgrade and commissioning period, the second observing run (O2) took place from November 30, 2016 to August 25, 2017. Advanced Virgo [6] joined this observing run on August 1, 2017. On April 1, 2019, Advanced LIGO and Advanced Virgo initiated their third observing run (O3), expected to last for one year [7]. The results of O1 and O2 include 11 confident detections (10 binary black hole mergers [4, 8–12] and 1 binary neutron star merger [13]) and 14 marginal triggers, collected and described in the Gravitational Wave Transient Catalog (GWTC-1) [14].

Notable events in this catalog are the first observed event GW150914 [4], the first three-detector event GW170814 [12] and the binary neutron star (BNS) coalescence GW170817 [13], detected a few days later. This latter event is the first case where gravitational and electromagnetic waves have been observed from a single source [15] offering a comprehensive and sequential description of the physical processes at play during and after the merger of two neutron stars.

Advanced LIGO and Advanced Virgo data are open to researchers outside the LIGO Scientific Collaboration and the Virgo Collaboration (LVC), and to a broader public that includes amateur scientists, students, etc. The roadmap for the data release is described in the LIGO Data Management Plan [16] and in the Memorandum of Understanding between Virgo and LIGO [17] (Attachment A, Sec. 2.9). The LVC releases segments of GW strain data around validated discoveries when those discoveries are published individually or in a catalog, such as GWTC-1 [18]. The release of the entire dataset of an observation run occurs after a period of internal use to validate and calibrate the data. The data related to both the O1 and O2 runs were released in January 2018 [19] and in February 2019 [20], respectively. The release of the bulk data for the first block of six months of O3 is currently scheduled for April 2021, and November 2021 for the second 6-month block.

This article focuses on the already-released data from the O1 and O2 runs. Public access to these data along with extensive documentation and usage instructions are provided through the Gravitational Wave Open Science Center (GWOSC) [21] at `http://gw-openscience.org`. GWOSC also provides online tools for finding and viewing data, usage guidelines and tutorials. We summarize this information, and include a comprehensive bibliography describing several aspects related to the production, characterization and analysis of these data.

To date over 80 scientific articles have been written using the data from the GWOSC website.[1] Some of these papers contain analyses of the released data by groups external to the LVC that have produced results consistent with the

[1] `http://gw-openscience.org/projects/`

LVC's [22–27]. A few extra event candidates have also been reported in [28–31]. The list of projects goes beyond published scientific research and also includes student projects, academic courses, and art installations.

This paper is organized as follows. The *Methods* section provides insights about how the data are collected and calibrated, about data quality and simulated signal injections. The GWOSC file format and content are described in the *Data records* section, while the *Usage notes* section gives suggestions on the tools that can be used to guide the analysis of the GW data.

Methods

The Advanced LIGO [5] and Advanced Virgo [6] detectors are enhanced Michelson interferometers (see a simplified description of the experimental layout in Fig. 3 of [4] and Fig. 3 of [6]). Each detector has two orthogonal arms of equal length $L_x = L_y = L$, each with two mirrors acting as test masses and forming a Fabry-Perot optical cavity. The arm length is $L = 4$ km for LIGO, and $L = 3$ km for Virgo. Advanced LIGO consists of two essentially identical detectors at Hanford, Washington and Livingston, Louisiana, while the Advanced Virgo detector is located in Cascina near Pisa, Italy.

When GWs reach Earth, they alter the detector arm lengths, stretching or contracting each one according to the wave's direction, polarization and phase. This induces a time-dependent differential arm length change $\Delta L = \delta L_x - \delta L_y = hL$, proportional to the GW strain amplitude h projected onto the detector (see e.g., [1] chap. 9, p. 470). Photodiodes continuously sense the differential length variations by measuring the interference between the two laser beams that return to the beam splitter from the detector arms.

While Advanced LIGO and Advanced Virgo follow a similar general scheme, each facility has a specific, though closely related, design. Both instruments are the result of major upgrades of initial detectors, that were in operation until 2011. We refer the reader to the following references for details about the technical upgrades to the instrumentation and instrument controls that were essential to reach the sensitivities obtained during the O1 and O2 observing runs.

For Advanced LIGO those include the light source (a pre-stabilized laser) [32, 33], the main optics [34–41], the signal recycling mirror (used to optimize the GW signal extraction) [5, 42, 43], the optics suspension and seismic isolation systems [44–57], the sensing and control strategies [58–60], the automation system [61], and various techniques for the mitigation of optical contamination, stray light and thermal effects [62–65].

For Advanced Virgo [6, 66] a similar list includes the high reflective coatings of the core optics [67, 68], the locking, control and thermal compensation systems [69–71], and the mitigation of magnetic and seismic noises [72–75].

When the detectors are taking data in their nominal configuration, they are said to be in *observing mode* or *science mode*. This condition does not occur all the time for various technical reasons. For example, the Fabry-Perot cavities included in the detector arms have to be kept at resonance together with the power and signal recycling cavities. There are periods when the control loops fail to maintain the instrument on this working point. There are also maintenance periods or conditions of excessive noise, due to bad weather conditions for instance.

The time percentage during which the detectors are in science mode is called *duty cycle* or *duty factor*. During O1 and O2, the individual LIGO detectors had duty factors of approximately 60%. If we define the *network duty factor* by the time percentage during which all the detectors in the network are in science mode simultaneously, the LIGO network duty factor was about 45%. When Virgo joined O2, it operated with an individual duty factor of about 80% [14].

It is customary to quantify the detector sensitivity by the *BNS range* [7, 76], defined as the distance to which a GW detector can register a GW signal from a BNS coalescence (assuming each neutron star with mass of 1.4 $M_{\odot}$) with a signal-to-noise ratio (SNR) of 8, averaged over all possible sky locations and orientations of the source. The sensitivities reached during O1 and O2 are shown in Figs. 1 and 2, together with the equivalent cumulative time-volume [76] obtained by multiplying the observed astrophysical volume by the amount of time spent observing. Note that these plots are indicative of the performance of the individual detector. However, observations are performed jointly by Advanced LIGO and Advanced Virgo as a network. Roughly speaking, the sensitivity of the global network is determined by that of the second most sensitive detector operating at any time. Despite the lower BNS range and cumulative time-volume for Virgo, its contribution has been important for astrophysical parameter estimation, especially in determining source localization and orientation [77]. Note, also, that the sensitive distance depends strongly on the system mass, and can be much higher (up to gigaparsecs) for higher-mass BBH systems (see e.g. Fig. 1 of Ref. [78]).

Calibration

The differential arm length read-out of the interferometer is recorded digitally through a dedicated data acquisition system [5, 6, 80]. The LIGO and Virgo data acquisition systems acquire the data at sampling rates $f_s = 16384$ Hz and 20000 Hz, respectively. The Virgo data is digitally converted to the same sampling rate as LIGO.

An elaborate calibration procedure [81–86] is applied to produce the dimensionless strain from the differential arm length read-out. For both the Advanced LIGO and Advanced Virgo detectors, the calibration procedure creates a digital time series, $h(t)$, from the detector control system channels. Details of the production and characterization of $h(t)$ can be found in [87, 88]. The calibration uncertainty estimation and residual systematic errors are discussed in [88–90]. The strain time series include both detector noise and any astrophysical signal that might be present.

Different versions of the calibrated data are available. The strain $h(t)$ is produced online using calibration parameters measured just before the observing

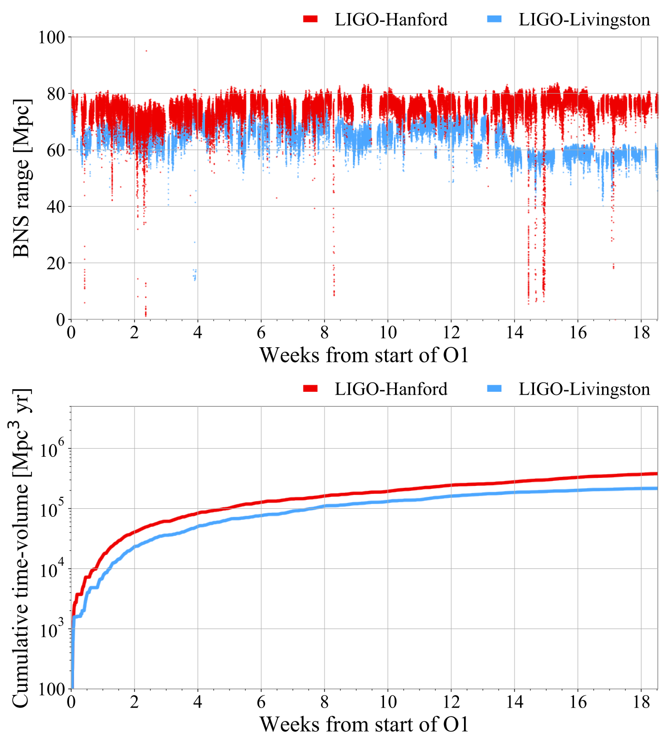

Figure 1: Upper plot: O1 sensitivity of the Livingston and Hanford detectors to GWs as measured by the BNS range (in megaparsecs) to binary neutron-star mergers averaged over all sky positions and source orientations [76, 79]. Lower plot: cumulative time-volume (assuming an Euclidean geometry appropriate for small redshifts) of the Livingston and Hanford detectors during O1, obtained by multiplying the observed astrophysical volume by the amount of time spent observing.

period starts. This data stream is analyzed within a few seconds to generate alerts when an event is detected thus allowing follow-up observations by other facilities[2] [91]. Another version of the calibration is produced later, offline, to include improvements to the calibration models or filters and to resolve dropouts in the initial online version. This process can be repeated leading to different offline calibration versions. The data provided to the public by GWOSC are obtained with the most recent calibration available at the time of the release. The calibration versions differ for the single event data releases depending on whether they pertain to the initial publication of the event (early version) [92–98] or to the catalog GWTC-1 publication (final version) [18].

The detector strain $h(t)$ is only calibrated between 10 Hz and 5000 Hz. The

[2]During the first and second observing runs, low-latency alerts were sent to external observers who had signed a memorandum of understanding with the LVC. They became public during the third observing run [7].

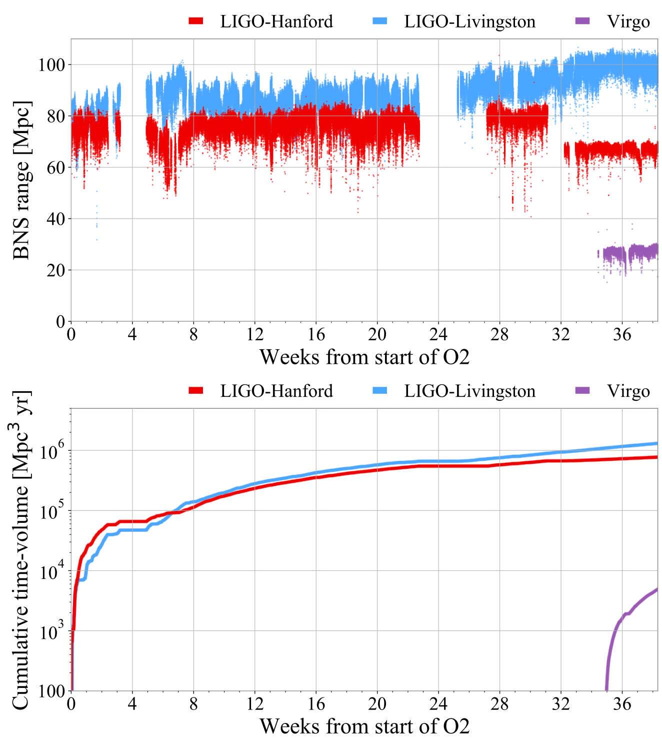

Figure 2: Upper plot: O2 sensitivity of the Livingston, Hanford and Virgo detectors to GWs as measured by the BNS range (in megaparsecs) to binary neutron-star mergers averaged over all sky positions and source orientations [76, 79]. Lower plot: cumulative time-volume (assuming an Euclidean geometry appropriate for small redshifts) of the Livingston, Hanford and Virgo detectors during O2, obtained by multiplying the observed astrophysical volume by the amount of time spent observing. Although Virgo has a lower BNS range and cumulative time-volume, its contribution is crucial for the source localization and the astrophysical parameter estimation.

apparent signal outside this range cannot be trusted because it is not a faithful representation of the GW strain at those frequencies [87, 89].

Detector noise characterization and data quality

The strain measurement is impacted by multiple noise sources, such as quantum sensing noise, seismic noise, suspension thermal noise, mirror coating thermal noise, and local gravity gradient noise produced by seismic waves (called Newtonian noise) [5]. In Figs. 3 and 4 the noise budget for O2 is shown for Advanced LIGO and Advanced Virgo, respectively. The plots show the measured noise spectrum and the contribution from various known noise sources.[3] The noise spectra indicate that the dominant noises rise steeply at high and low frequencies, thus drastically reducing the chance for observing GWs in those parts of the spectrum. This opens an observational window between tens of Hz and a few kHz. Search pipelines usually concentrate on frequency intervals smaller than the full calibrated bandwidth to avoid the high noise level at the extremes of this band.

The strain data are band-pass filtered between 10 Hz and 5000 Hz to avoid a number of digital signal processing problems related to spectral dynamic range and floating point precision limitation, or aliasing [100] that may occur downstream when searching in the data.

The data contain spectral peaks, or lines, that can complicate searches for signals in those frequency bands. These lines include calibration lines, power line harmonics, "violin" modes (resonant frequencies of mirror suspension fibers), other known instrumental lines, unknown lines and also evenly spaced combs of narrow lines, typically in exact multiples of some fundamental frequency. Further details on spectral lines during O1 and O2 can be found in [102, 103] as well as on the GWOSC web pages.[4]

The detector sites are equipped with about ten thousand sensors that monitor both the instrumental and environmental state [104]. The measurements performed by these sensors are recorded in *auxiliary channels* that are crucial for diagnosing instrument faults or for identifying environmental perturbations. Non-Gaussian transient noise artifacts, called glitches, can mask or mimic true astrophysical signals [105]. Auxiliary channels provide a useful source of information for the characterization of glitches, and their mitigation. Glitches are caused by anomalous behavior in instrumental or environmental channels that couple into the GW channel. The observation of coincident glitches between the GW and auxiliary channels provides a mechanism for rejecting a detected event in the former as not astrophysical in origin. *Data quality vetoes* generated from auxiliary channels allow identification of times that are unsuitable for analysis or are likely to produce false alarms. Veto conditions are determined using systematic studies to remove glitches with high efficiency and limited loss of

[3] For similar noise budget plots for O1 see also [42]. Other useful references for the detector sensitivity are [99] for O1 and [14] for O2.

[4] `http://gw-openscience.org/o1speclines` and `http://gw-openscience.org/o2speclines`

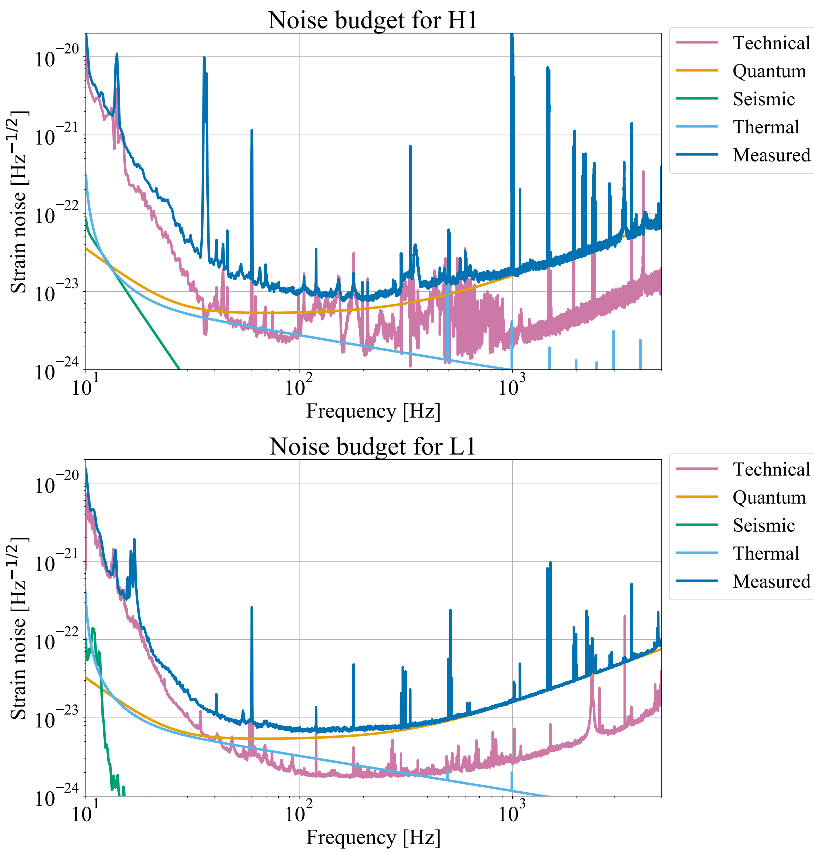

Figure 3: Sensitivities of the Advanced LIGO detectors during the second observation run (O2), expressed as the equivalent strain noise spectrum of each detector (the blue "Measured" curves). Also shown are the known contributors to the detector noise, which sum to the measured spectrum across much, but not all of the frequency band (i. e. the measured noise spectrum is not fully explained by all known sources of noise). The quantum noise includes both shot noise (dominant at higher frequencies) and radiation pressure noise (dominant at lower frequencies). Thermal noise includes contributions from the suspensions, the substrate and coatings of the test masses. Seismic noise is computed as the ground displacement attenuated through the seismic isolation system and the suspensions chain. The seismic curves differ for H1 and L1 as actual seismic data were used for L1 while the H1 curve is a model that also includes Newtonian noise. Technical noise includes angular and length sensing/control noise for degrees of freedom that are not related to the differential arm length measurement, and other sub-dominant noises such as laser frequency, intensity and beam jitter noise, sensor and actuation noise, and Rayleigh scattering by the residual gas. The strong line features are due to the violin modes of the suspension wires, other resonance modes of the suspensions, the AC power line and its harmonics, and the calibration lines. Examples of similar plots for other data taking runs can be found in [42, 101]. These noise spectra do not include any of the post-data collection noise subtraction mentioned in the text.

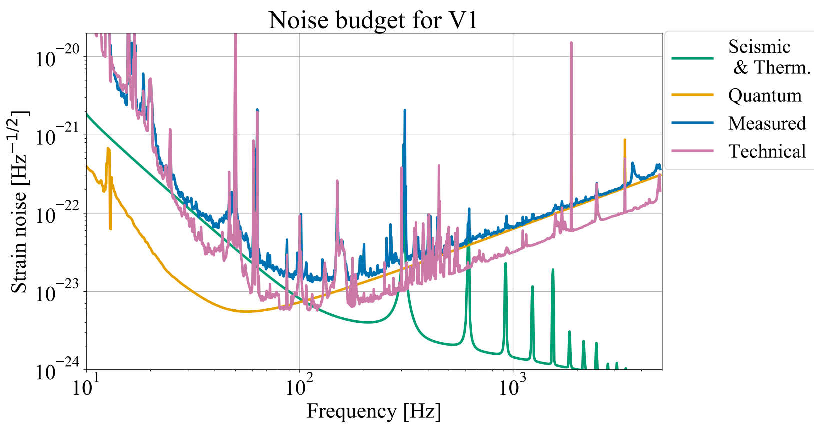

Figure 4: Sensitivity of the Advanced Virgo detector during the O2 observation run. The meaning of the noise source contributions is the same as in Fig. 3, except for the seismic and thermal noises that are combined in this case and for the Newtonian noise which is not included. These noise spectra do not include any of the post-data collection noise subtraction mentioned in the text.

observation time [105]. As an example, vetoes discard glitches from electronics faults, photodiode saturations, analog-to-digital converter (ADC) and digital-to-analog converter (DAC) overflows, elevated seismic noise and computer failures. They are used by the GW searches to reduce the noise background [105].

Different categories of data quality are defined according to the severity level and degree of understanding of the noise artifact. Data flagged as invalid due to severe detector malfunctioning, calibration error, or data acquisition problems, as described in [106] are typically not used for data analysis and are replaced by `NaN`s in the GWOSC data releases. We elaborate further on the various data quality categories and their usage in the *Data records* section.[5]

Auxiliary channels are also used to subtract post-facto some well identified instrumental noise from the GW strain data. A procedure based on a linear coupling model [107] computes the transfer function that couples the witness channels to $h(t)$ and subtracts the contributing noise from the strain amplitude. This procedure was used during the second observing run in Advanced LIGO data. It achieved an increase of up to 30% of the detector sensitive volume to GWs for a broad range of compact binary systems and was most significant for the LIGO-Hanford detector [108]. In some cases data are available both before and after noise subtraction is applied (for example in the case of GW170817 [98]).

[5]See also `http://gw-openscience.org/o1_details` and `http://gw-openscience.org/o2_details`

Signal injections

In addition to data quality, some metadata provide information about *hardware injections* [109], i.e. simulated GW signals inserted into the detector data for testing and calibration. The detectors' test masses (interferometer mirrors) are physically displaced by an actuator in order to simulate the effects of a GW. The simulated signal is introduced into the detector control system yielding a response which mimics that of a true GW. The analysis of a data segment that includes an injection allows an end-to-end test of the ability for the analysis procedure to detect and characterize the GW strain signal. Hardware injections are also used for detector characterization to check that the auxiliary channels used for vetoes do not respond to gravitational-wave-like signals. This is a *safety* check since a channel that has no sensitivity to GWs is considered safe for use when constructing a veto. It is clearly important to keep a record of injections to avoid any confusion with real events. In the *Data records* section we describe how this bookkeeping is done.[6]

Data records

GW open data are distributed under the Creative Commons attribution international public license 4.0[7] through the GWOSC web pages.[8] The files can be directly downloaded one by one from this web page. However, to download large amounts of data (as in the case of a whole observing run) the use of the distributed filesystem `CernVM-FS` is preferred.[9] Once installed, this filesystem allows access to GWOSC data as files in a directory tree mounted locally on the user's computer.

Segments of 32 s and 4096 s duration, to the extent possible, are released for each GW event while the strain data from full observation runs are conveniently divided into files of 4096 s. The description of the data records that follows is valid both for single event release and for bulk data release.

The strain data are repackaged and resampled by GWOSC to make it more accessible to users both within the LVC and outside. Along with the native 16384 Hz sampling rate, the data on GWOSC are also made available at 4096 Hz.[10] The down-sampling is performed using the standard decimation technique implemented in `scipy.signal.decimate`[11] from the Python package `scipy` [111]. From the Nyquist-Shannon sampling theorem [112–114], the largest accessible frequency is the Nyquist frequency equal to half of the sampling rate f_s. This should be kept in mind when choosing the sampling rate to download

[6] See the GWOSC web page `http://gw-openscience.org/o1_inj` and `http://gw-openscience.org/o2_inj`

[7] `https://creativecommons.org/licenses/by/4.0/legalcode`

[8] `http://gw-openscience.org/data/`

[9] For installation instructions, see `http://gw-openscience.org/cvmfs/`

[10] In the rest of the paper the sampling rates will be indicated in kHz and rounded to the closest integer, i.e. 4 and 16 kHz means 4096 and 16384 Hz, respectively

[11] This method applies an anti-aliasing filter based on an order-8 Chebychev type I infinite impulse response (IIR) filter [110] before decimation.

from GWOSC, and in general when analyzing these files; in particular, because of the anti-aliasing filter's roll-off, the data sampled at 4 kHz are valid only up to frequencies of about 1700 Hz.

The publicly released data are generated from data streams in the LIGO and Virgo data archives uniquely identified by a channel name and a frame type (an internal label that specifies the content of the files). For completeness, we give the provenance of the GWOSC data in Table 1 and list the channel names and frame types used to generate the O1 and O2 dataset discussed in this article. In this table and in the following, H1 and L1 indicate the two LIGO detectors (Hanford and Livingston respectively) while V1 refers to Virgo. Downsampling (for the 4 kHz dataset) and replacement with `NaN`s of bad quality or absent data are the only modification of the original data.

Table 1: The channel names and frame types listed in this table are unique identifiers in the LIGO and Virgo data archives that allow tracing the provenance of the strain data released on GWOSC. The attribute `CLEAN` in H1 and L1 for O2 indicates that the noise subtraction procedure mentioned previously and described in [107] was used. The attributes `C02` and `Repro2A` refer to the calibration version.

Run	Det.	Channel name	Frame type
O1	H1	`H1:DCS-CALIB_STRAIN_C02`	`H1_HOFT_C02`
O1	L1	`L1:DCS-CALIB_STRAIN_C02`	`L1_HOFT_C02`
O2	H1	`H1:DCH-CLEAN_STRAIN_C02`	`H1_CLEANED_HOFT_C02`
O2	L1	`L1:DCH-CLEAN_STRAIN_C02`	`L1_CLEANED_HOFT_C02`
O2	V1	`V1:Hrec_hoft_V1O2Repro2A_16384Hz`	`V1O2Repro2A`

GWOSC file formats

The GW open data are delivered in two different file formats: `hdf` and `gwf`. The Hierarchical Data Format `hdf` [115] is a portable data format readable by many programming languages. The Frame format `gwf` [116] is used internally by the GW community. In addition, the data associated with GW events are also released as plain text files containing two columns with the time and the corresponding strain values.

The `hdf` files contain:

- *Metadata*: description of the data, URL of the GWOSC website, detector and observatory concerned, duration of the segment of data, starting time both in GPS and UTC.
- *Strain*: $h(t)$, sampled at 4 or 16 kHz depending on the file, and accompanied by some attributes such as the starting GPS time, the sampling step in the time series and the number of samples. For the times when the detector is not in science mode or the data does not meet the minimum required data quality conditions (see next section), the strain values are set to `NaN`s.

- *Quality*: 1-Hz time series that encode the data quality information recommended to use for GW searches. This also includes a 1-Hz time series that flags hardware injections, that were introduced in the *Data records* section.

The `gwf` files contain the same information with one channel for the strain data, one for the data quality and one for the injections. The channel names slightly differ in O1 and O2 as described in Table 2.

Table 2: Channel names of the GWOSC frame (`gwf`) files. In the name, *ifo* is a place holder for the interferometer name, i.e. H1, L1 or V1, and *s* the sampling rate in kHz. The `R1` substring represents the revision number of the channel name so it will become `R2` in case there is a second (revised) release, and so on.

O1 (4 kHz sampling)	O1 (16 kHz sampling) and O2
ifo:`LOSC-STRAIN`	*ifo*:`GWOSC-`*s*`KHZ_R1_STRAIN`
ifo:`LOSC-DQMASK`	*ifo*:`GWOSC-`*s*`KHZ_R1_DQMASK`
ifo:`LOSC-INJMASK`	*ifo*:`GWOSC-`*s*`KHZ_R1_INJMASK`

Data quality and injections in GWOSC files

Several types of searches are performed on the LIGO and Virgo data. Those searches are divided into four families named after the type of signals they target: Compact binary coalescences (`CBC`), GW bursts (`BURST`), continuous waves (`CW`) and stochastic backgrounds (`STOCH`).

`CBC` analyses (see e.g., [8, 14, 78, 117–121]) seek signals from merging neutron stars and black holes by filtering the data with waveform templates. `BURST` analyses (see e.g., [122–126]) search for generic GW transients with minimal assumption on the source or signal morphology by identifying excess power in the time-frequency representation of the GW strain data. `CW` searches (see e.g., [127–130]) look for long-duration, continuous, periodic GW signals from asymmetries of rapidly spinning neutron stars. `STOCH` searches (see e.g., [131, 132]) target the stochastic GW background signal which is formed by the superposition of a wide variety of independent and unresolved sources from different stages of the evolution of the Universe.

Due to the fundamental differences among these searches, some types of noise are problematic only for one or two types of search. For this reason, the data quality related to transient noises depends on the search type. It is provided inside the GWOSC files for the two GW transient searches `CBC` and `BURST`, that are most sensitive to this type of noise. The data quality information most relevant for `CW` and `STOCH` searches is in the frequency domain and it is provided as lists of instrumental lines in separate files [133–137].

Data quality and signal injection information for a given GPS second is indicated by bitmasks with a 1-Hz sampling rate. The bit meanings are given in Tables 3 and 4 for the data quality and injections, respectively. To describe data quality, different *categories* are defined. For each category, the corresponding bit in the bitmask shown in Table 3 has value 1 (good data) if in that second of time the requirements of the category are fulfilled, otherwise 0 (bad data). The meaning of each category is the following:

`DATA` Failing this level indicates that LIGO and Virgo data are not available in GWOSC data because the instruments were not operating in nominal conditions. For O1 and O2, this is equivalent to failing Category 1 criteria, defined below. For these seconds of bad or absent data, `NaN`s have been inserted.

`CAT1` (Category 1) Failing a data quality check at this category indicates a critical issue with a key detector component not operating in its nominal configuration. Since these times indicate a major known problem these times are identical for each data analysis group. However, while `CBC_CAT1` and `BURST_CAT1` flag the same data, they exist separately in the dataset. GWOSC data during times that fail CAT1 criteria are replaced by `NaN` values in the strain time series. The time lost due to these critical quality issues (*dead time*) is: 1.683% (H1) and 1.039% (L1) of the run during O1; and 0.001% (H1), 0.003% (L1) and 0.053% (V1) of the run during O2 (all the percentages have been calculated with respect to the periods of science mode).

`CAT2` (Category 2) Failing a data quality check at this category indicates times when there is a known, understood physical coupling between a sensor/auxiliary channel that monitors excess noise, and the strain channel. The dead times corresponding to this veto for the `CBC` analysis are: 0.890% (H1) and 0.007% (L1) of the run during O1; 0.157% (H1) and 0.090% (L1) of the run during O2. The dead times corresponding to this veto for the `BURST` analysis are: 0.624% (H1) and 0.021% (L1) of the run during O1; 0.212% (H1) and 0.151% (L1) of the run during O2. `CAT2` was not used for Virgo in O2.

`CAT3` (Category 3) Failing a data quality check at this category indicates times when there is statistical coupling between a sensor/auxiliary channel and the strain channel which is not fully understood. This category was not used in O1 and O2 LVC searches, but it is still in the file format for historical reasons.

Data quality categories are cascading: a time which fails a given category automatically fails all higher categories. For example, if the only known problem with a given time fails the `BURST` category 2, then the data is said to pass `DATA` and `BURST_CAT1`, but fails `BURST_CAT2` and `BURST_CAT3`. However, the different analysis groups qualify the data independently: failing `BURST_CAT2` does not necessarily imply failing `CBC_CAT2`.

The various sensors/auxiliary channels used to define these categories are described in Ref. [138].

Table 3: Data quality bitmasks description. Data that are *not* present are replaced by `NaN` values in the strain time series. `CBC_CAT1` and `BURST_CAT1` are equivalent (see the definition of `CAT1` in the text).

Bit	Short name	Description
0	`DATA`	Data present
1	`CBC_CAT1`	Pass `CAT1` test
2	`CBC_CAT2`	Pass `CAT1` and `CAT2` test for `CBC` searches
3	`CBC_CAT3`	Pass `CAT1` and `CAT2` and `CAT3` test for `CBC` searches
4	`BURST_CAT1`	Pass `CAT1` test
5	`BURST_CAT2`	Pass `CAT1` and `CAT2` test for `BURST` searches
6	`BURST_CAT3`	Pass `CAT1` and `CAT2` and `CAT3` test for `BURST` searches

The injection bitmask marks the injection-free times. Five different types of injections are usually performed: injections simulating signals searched for by `CBC`, `BURST`, `CW` and `STOCH` LVC pipelines, and injections used for detector characterization labeled `DETCHAR`. For each injection type, the bit of the bitmask, whose meaning is described in Table 4, has value 1 if the injection is not present, otherwise 0.

Virgo did not perform hardware injections during O2, therefore all the bits of the injection bitmask have value 1.

Table 4: Meaning of the injection bits

Bit	Short name	Description
0	`NO_CBC_HW_INJ`	No `CBC` injections
1	`NO_BURST_HW_INJ`	No burst injections
2	`NO_DETCHAR_HW_INJ`	No detector characterization injections
3	`NO_CW_HW_INJ`	No continuous wave injections
4	`NO_STOCH_HW_INJ`	No stochastic injections

Technical Validation

The calibration of LIGO and Virgo data is reviewed and validated by an internal team of experts [81–84]. Similarly, the data repackaged for public use are also validated by another independent internal team. In particular, this review team checks that:

- the strain vector in the GWOSC `hdf` and `gwf` files exactly matches that of the files in the LIGO and Virgo main archives;
- the data quality and injection timestamp segments in the GWOSC files and in the visual representation of the segments provided by the GWOSC

website (the *Timeline* described in detail in the *Usage notes* section) are identical and correspond to what is included in the original data quality database developed by the LIGO and Virgo data quality experts;

- the documentation web pages and the content of the present article contain correct and comprehensive information.

The data files, the *Timeline* and the web pages are released to the public once all those checks have been passed.

Usage notes

GW detectors are complex instruments, and their data reflect this complexity. For this reason, caution should be taken when searching for GW signals in the detector strain data, taking into account all the details about the usable frequency range, noise artifacts, data quality and injections discussed in this paper and in the references. In particular, the application of all data quality flags described in the previous section does *not* imply that the remaining data are free of transient noise artifacts. Along with basic information about the data and the detectors, such as their geographical position[12] and their current status,[13] the GWOSC website contains useful tutorials and tools to help conduct an analysis properly, as described in the next sections. The data analysis techniques used to detect GW signals and infer the source properties are also described in a paper recently published by the LVC [100].

Timeline

The LIGO and Virgo detectors are not always in observing mode and, even when they are, it is possible that data quality does not meet the requirements of a given analysis. For these reasons it is necessary to restrict analysis to valid *segments* of data characterized by data quality information that indicates the data is acceptable for the desired analysis. *Timeline*[14] is a tool to provide a visual representation of available valid data segments over a time interval, together with the related information about data quality and presence of injected signals. If the requested interval is short enough, this is shown at the time scale of seconds. For longer intervals, *Timeline* shows the average value of the selected data-quality bit over nonoverlapping 2^n-second subintervals. From the *Timeline* page it is possible to select specific segments and download the corresponding data (see Fig. 5 for an example with the O2 dataset).

[12] `http://gw-openscience.org/static/param/position.txt`
[13] `http://gw-openscience.org/detector_status/`
[14] `http://gw-openscience.org/timeline/`

Figure 5: The GWOSC offers immediate access to duty cycle information for data quality and injection bits through the *Timeline*. By default, the time resolution is chosen to display the entire dataset. From there, one can zoom in to smaller timescales by clicking on the display.

Courses, software packages and tutorials for GW data analysis

On-line courses that provide an introduction to GW data analysis ranging from the basics to more advanced topics with hands-on exercices are available on the GWOSC website.[15] Those courses have been recorded at the GW Open Data Workshops. Two such workshops have been organized — in 2018 and 2019 [139]. The courses are supported by many tutorials[16] that can be used to understand how to read and analyze the data. Lectures on various aspects of GW science are also available.

A series of `Jupyter` notebooks [140] explain how to access the data, produce time-frequency spectrograms, carry out matched-filtering searches, infer astrophysical parameters, and manipulate GW localization information. A few tutorials start from first principles and use generic and broadly used analysis software such as `scipy` [111], but most are based on the specialized software packages and libraries that the LVC developed to produce observational results and other scientific products.

A list of those packages is available on the GWOSC website[17] and includes:

[15] See also `https://www.youtube.com/channel/UC8kOaTeQhqv7eKhP8Ynu--A`
[16] `http://gw-openscience.org/tutorials/`
[17] `http://gw-openscience.org/software/`

- the light-weight application `readligo` to access data;
- general purpose application software, such as the LSC Algorithm Library Suite (`LALSuite`) [141] and the Python package `gwpy` [142];
- search-oriented software such as `pycbc` [117, 118], `GstLAL` [143] and Coherent Waveburst (`cWB`) [122];
- post-processing software for e.g., parameter estimation such as `bilby` [144], `LALInference` [145] and Bayeswave [146, 147].

All these packages are open source and freely distributed.

Summary and additional information

The LVC is committed to providing strain data from the LIGO and Virgo detectors to the public, according to the schedule outlined in the LIGO Data Management Plan [16], via the Gravitational Wave Open Science Center GWOSC [148]. They are also committed to providing a broad range of data analysis products to facilitate reproducing the results presented in their observational papers. Many of these data products are available through the LIGO Document Control Center (DCC); for example, data products associated with the GWTC-1 event catalog [14] can be found in [18] and [149]. Many more, and improved, data offerings are planned for the future. This includes the catalog of observed events and the bulk strain data from the LIGO/Virgo O3 run. More GWOSC Open Data Workshops [139] are also planned.

All users of these data are welcome to sign up with the GWOSC User's Group at `https://www.gw-openscience.org/join/`. Anyone who uses these data in publications and other public data products are requested to acknowledge GWOSC by following the guidance in [150]. Publications that acknowledge GWOSC will be listed in `https://www.gw-openscience.org/projects/`; email `gwosc@igwn.org` to make sure your publication(s) are included.

The Collaborations, and the GWOSC team, welcome comments and suggestions for improving these data releases and products, and their presentation on the GWOSC website [148], via email to `gwosc@igwn.org`. Questions about the use of these data products may also be sent to that email, and will be entered into our help ticket system. More general questions about LIGO, Virgo, and GW science should go to `questions@ligo.org`.

Acknowledgements

This research has made use of data, software and/or web tools obtained from the Gravitational Wave Open Science Center (`https://www.gw-openscience.org`), a service of LIGO Laboratory, the LIGO Scientific Collaboration and the Virgo Collaboration. LIGO is funded by the U.S. National Science Foundation. Virgo is funded by the French Centre National de Recherche Scientifique

(CNRS), the Italian Istituto Nazionale della Fisica Nucleare (INFN) and the Dutch Nikhef institute, with contributions by Polish and Hungarian institutes.

The authors gratefully acknowledge the support of the United States National Science Foundation (NSF) for the construction and operation of the LIGO Laboratory and Advanced LIGO as well as the Science and Technology Facilities Council (STFC) of the United Kingdom, the Max-Planck-Society (MPS), and the State of Niedersachsen/Germany for support of the construction of Advanced LIGO and construction and operation of the GEO600 detector. Additional support for Advanced LIGO was provided by the Australian Research Council. The authors gratefully acknowledge the Italian Istituto Nazionale di Fisica Nucleare (INFN), the French Centre National de la Recherche Scientifique (CNRS) and the Foundation for Fundamental Research on Matter supported by the Netherlands Organisation for Scientific Research, for the construction and operation of the Virgo detector and the creation and support of the EGO consortium. The authors also gratefully acknowledge research support from these agencies as well as by the Council of Scientific and Industrial Research of India, the Department of Science and Technology, India, the Science & Engineering Research Board (SERB), India, the Ministry of Human Resource Development, India, the Spanish Agencia Estatal de Investigación, the Vicepresidència i Conselleria d'Innovació, Recerca i Turisme and the Conselleria d'Educació i Universitat del Govern de les Illes Balears, the Conselleria d'Educació, Investigació, Cultura i Esport de la Generalitat Valenciana, the National Science Centre of Poland, the Swiss National Science Foundation (SNSF), the Russian Foundation for Basic Research, the Russian Science Foundation, the European Commission, the European Regional Development Funds (ERDF), the Royal Society, the Scottish Funding Council, the Scottish Universities Physics Alliance, the Hungarian Scientific Research Fund (OTKA), the Lyon Institute of Origins (LIO), the Paris Île-de-France Region, the National Research, Development and Innovation Office Hungary (NKFIH), the National Research Foundation of Korea, Industry Canada and the Province of Ontario through the Ministry of Economic Development and Innovation, the Natural Science and Engineering Research Council Canada, the Canadian Institute for Advanced Research, the Brazilian Ministry of Science, Technology, Innovations, and Communications, the International Center for Theoretical Physics South American Institute for Fundamental Research (ICTP-SAIFR), the Research Grants Council of Hong Kong, the National Natural Science Foundation of China (NSFC), the Leverhulme Trust, the Research Corporation, the Ministry of Science and Technology (MOST), Taiwan and the Kavli Foundation. The authors gratefully acknowledge the support of the NSF, STFC, INFN and CNRS for provision of computational resources.

Competing interests

No conflict of interest

References

[1] Maggiore, M. *Gravitational Waves, volume 1: theory and experiments* (Oxford University Press, 2008).

[2] Einstein, A. Approximative Integration of the Field Equations of Gravitation. *Sitzungsber. Preuss. Akad. Wiss. Berlin (Math. Phys.)* **1916**, 688–696 (1916).

[3] Einstein, A. Über Gravitationswellen. *Sitzungsber. Preuss. Akad. Wiss. Berlin (Math. Phys.)* **1918**, 154–167 (1918).

[4] Abbott, B. P. *et al.* (LIGO Scientific Collaboration, Virgo Collaboration). Observation of gravitational waves from a binary black hole merger. *Phys. Rev. Lett.* **116**, 061102 (2016).

[5] Aasi, J. *et al.* (LIGO Scientific Collaboration). Advanced LIGO. *Class. Quantum Grav.* **32**, 074001 (2015).

[6] Acernese, F. *et al.* (Virgo Collaboration). Advanced Virgo: a second-generation interferometric gravitational wave detector. *Class. Quantum Grav.* **32**, 024001 (2015).

[7] KAGRA Collaboration, LIGO Scientific Collaboration, and Virgo Collaboration. Prospects for observing and localizing gravitational-wave transients with Advanced LIGO, Advanced Virgo and KAGRA (2019). Preprint at `https://arxiv.org/abs/1304.0670`.

[8] Abbott, B. P. *et al.* (LIGO Scientific Collaboration, Virgo Collaboration). GW150914: First Results from the Search for Binary Black Hole Coalescence with Advanced LIGO. *Phys. Rev. D* **93**, 122003 (2016).

[9] Abbott, B. P. *et al.* (LIGO Scientific Collaboration, Virgo Collaboration). GW151226: Observation of Gravitational Waves from a 22-Solar-Mass Binary Black Hole Coalescence. *Phys. Rev. Lett.* **116**, 241103 (2016).

[10] Abbott, B. P. *et al.* (LIGO Scientific Collaboration, Virgo Collaboration). Binary Black Hole Mergers in the First Advanced LIGO Observing Run. *Phys. Rev. X* **6**, 041015 (2016).

[11] Abbott, B. P. *et al.* (LIGO Scientific Collaboration, Virgo Collaboration). GW170104: Observation of a 50-Solar-Mass Binary Black Hole Coalescence at Redshift 0.2. *Phys. Rev. Lett.* **118**, 221101 (2017).

[12] Abbott, B. P. *et al.* (LIGO Scientific Collaboration, Virgo Collaboration). GW170814: A Three-Detector Observation of Gravitational Waves from a Binary Black Hole Coalescence. *Phys. Rev. Lett.* **119**, 141101 (2017).

[13] Abbott, B. P. *et al.* (LIGO Scientific Collaboration, Virgo Collaboration). GW170817: Observation of Gravitational Waves from a Binary Neutron Star Inspiral. *Phys. Rev. Lett.* **119**, 161101 (2017).

[14] Abbott, B. P. *et al.* (LIGO Scientific Collaboration, Virgo Collaboration). GWTC-1: A Gravitational-Wave Transient Catalog of Compact Binary Mergers Observed by LIGO and Virgo during the First and Second Observing Runs. *Phys. Rev. X* **9**, 031040 (2019). `arXiv:1811.12907`.

[15] Abbott, B. P. *et al.* Multi-messenger observations of a binary neutron star merger. *ApJ* **848**, L12 (2017).

[16] Anderson, S. & Williams, R. LIGO Data Management Plan (2017). URL `https://dcc.ligo.org/LIGO-M1000066/public`.

[17] LIGO Scientific Collaboration and Virgo Collaboration. Memorandum of understanding between Virgo and LIGO (2019). LIGO-M060038, VIR-0091A. `https://dcc.ligo.org/LIGO-M060038/public`.

[18] LIGO Scientific Collaboration and Virgo Collaboration. LIGO/Virgo GWTC-1 Data Release (2018). URL `https://www.gw-openscience.org/GWTC-1/`.

[19] LIGO Scientific Collaboration and Virgo Collaboration. LIGO/Virgo O1 Data Release (2018). URL `https://www.gw-openscience.org/O1/`.

[20] LIGO Scientific Collaboration and Virgo Collaboration. LIGO/Virgo O2 Data Release (2019). URL `https://www.gw-openscience.org/O2/`.

[21] Vallisneri, M., Kanner, J., Williams, R., Weinstein, A. & Stephens, B. The LIGO Open Science Center. *J. Phys. Conf. Ser.* **610**, 012021 (2015). `arXiv:1410.4839`.

[22] Green, M. A. & Moffat, J. W. Extraction of black hole coalescence waveforms from noisy data. *Phys. Lett. B* **784**, 312 (2018). `arXiv:1711.00347`.

[23] Nielsen, A. B., Nitz, A. H., Capano, C. D. & Brown, D. A. Investigating the noise residuals around the gravitational wave event GW150914. *JCAP* **1902**, 019 (2019). `arXiv:1811.04071`.

[24] Radice, D. & Dai, L. Multimessenger Parameter Estimation of GW170817. *Eur. Phys. J. A* **55**, 50 (2019). `arXiv:1810.12917`.

[25] De, S. *et al.* Tidal Deformabilities and Radii of Neutron Stars from the Observation of GW170817. *Phys. Rev. Lett.* **121**, 091102 (2018). `arXiv:1804.08583`.

[26] De, S., Capano, C. D., Biwer, C. M., Nitz, A. H. & Brown, D. A. Posterior samples of the parameters of binary black holes from Advanced LIGO, Virgo's second observing run. *Scientific Data* **6**, 81 (2019). `arXiv:1811.09232`.

[27] Nitz, A. H. *et al.* 1-OGC: The first open gravitational-wave catalog of binary mergers from analysis of public Advanced LIGO data. *Astrophys. J.* **872**, 195 (2019). `arXiv:1811.01921`.

[28] Zackay, B., Venumadhav, T., Dai, L., Roulet, J. & Zaldarriaga, M. A Highly Spinning and Aligned Binary Black Hole Merger in the Advanced LIGO First Observing Run. *Phys. Rev. D* **100**, 023007 (2019). arXiv:1902.10331.

[29] Venumadhav, T., Zackay, B., Roulet, J., Dai, L. & Zaldarriaga, M. New Binary Black Hole Mergers in the Second Observing Run of Advanced LIGO and Advanced Virgo (2019). Preprint at https://arxiv.org/abs/1904.07214.

[30] Nitz, A. H. *et al.* 2-OGC: Open Gravitational-wave Catalog of binary mergers from analysis of public Advanced LIGO and Virgo data (2019). Preprint at https://arxiv.org/abs/1910.05331.

[31] Zackay, B., Dai, L., Venumadhav, T., Roulet, J. & Zaldarriaga, M. Detecting Gravitational Waves With Disparate Detector Responses: Two New Binary Black Hole Mergers (2019). Preprint at https://arxiv.org/abs/1910.09528.

[32] Kwee, P. *et al.* Stabilized high-power laser system for the gravitational wave detector Advanced LIGO. *Opt. Express* **20**, 10617–10634 (2012). URL https://doi.org/10.1364/OE.20.010617.

[33] Winkelmann, L. *et al.* Injection-locked single-frequency laser with an output power of 220 W. *Appl. Phys. B* **102**, 529 – 538 (2011). URL https://doi.org/10.1007/s00340-011-4411-9.

[34] Liu, Z. *et al.* Feedback control of optical beam spatial profiles using thermal lensing. *Appl. Opt.* **52**, 6452–6457 (2013). URL https://doi.org/10.1364/AO.52.006452.

[35] Palashov, O. V. *et al.* High-vacuum-compatible high-power faraday isolators for gravitational-wave interferometers. *J. Opt. Soc. Am. B* **29**, 1784–1792 (2012). URL https://doi.org/10.1364/JOSAB.29.001784.

[36] Dooley, K. L. *et al.* Thermal effects in the input optics of the enhanced laser interferometer gravitational-wave observatory interferometers. *Rev. Sci. Instrum.* **83** (2012). URL https://doi.org/10.1063/1.3695405.

[37] Arain, M. A. & Mueller, G. Design of the Advanced LIGO recycling cavities. *Opt. Express* **16**, 10018–10032 (2008). URL http://www.opticsexpress.org/abstract.cfm?URI=oe-16-14-10018.

[38] Mueller, C. L. *et al.* The Advanced LIGO input optics. *Rev. Sci. Instrum.* **87**, 014502 (2016). URL http://scitation.aip.org/content/aip/journal/rsi/87/1/10.1063/1.4936974.

[39] Harry, G. M. *et al.* Titania-doped tantala/silica coatings for gravitational-wave detection. *Class. Quantum Grav.* **24**, 405 (2007). URL http://stacks.iop.org/0264-9381/24/i=2/a=008.

[40] Granata, M. *et al.* Mechanical loss in state-of-the-art amorphous optical coatings. *Phys. Rev. D* **93**, 012007 (2016). URL https://doi.org/10.1103/PhysRevD.93.012007.

[41] Pinard, L. *et al.* Mirrors used in the LIGO interferometers for first detection of gravitational waves. *Appl. Opt.* **56**, C11 (2017). URL https://doi.org/10.1364/AO.56.000C11.

[42] Abbott, B. P. *et al.* (LIGO Scientific Collaboration, Virgo Collaboration). GW150914: The Advanced LIGO detectors in the era of first discoveries. *Phys. Rev. Lett.* **116**, 131103 (2016). URL http://link.aps.org/doi/10.1103/PhysRevLett.116.131103.

[43] Buonanno, A. & Chen, Y. Signal recycled laser-interferometer gravitational-wave detectors as optical springs. *Phys. Rev. D* **65**, 042001 (2002). URL https://link.aps.org/doi/10.1103/PhysRevD.65.042001.

[44] Heptonstall, A. *et al.* Enhanced characteristics of fused silica fibers using laser polishing. *Class. Quantum Grav.* **31**, 105006 (2014). URL http://stacks.iop.org/0264-9381/31/i=10/a=105006.

[45] Bell, C. J. *et al.* Experimental results for nulling the effective thermal expansion coefficient of fused silica fibres under a static stress. *Class. Quantum Grav.* **31**, 065010 (2014). URL http://stacks.iop.org/0264-9381/31/i=6/a=065010.

[46] Tokmakov, K. *et al.* A study of the fracture mechanisms in pristine silica fibres utilising high speed imaging techniques. *J. Non Cryst. Solids* **358**, 1699 – 1709 (2012). URL http://www.sciencedirect.com/science/article/pii/S0022309312002554.

[47] Hammond, G. D. *et al.* Reducing the suspension thermal noise of advanced gravitational wave detectors. *Class. Quantum Grav.* **29**, 124009 (2012). URL http://stacks.iop.org/0264-9381/29/i=12/a=124009.

[48] Aston, S. M. *et al.* Update on quadruple suspension design for Advanced LIGO. *Class. Quantum Grav.* **29**, 235004 (2012). URL http://stacks.iop.org/0264-9381/29/i=23/a=235004.

[49] Carbone, L. *et al.* Sensors and actuators for the Advanced LIGO mirror suspensions. *Class. Quantum Grav.* **29**, 115005 (2012). URL http://stacks.iop.org/0264-9381/29/i=11/a=115005.

[50] Cumming, A. V. *et al.* Design and development of the Advanced LIGO monolithic fused silica suspension. *Class. Quantum Grav.* **29**, 035003 (2012). URL http://stacks.iop.org/0264-9381/29/i=3/a=035003.

[51] Heptonstall, A. *et al.* Invited article: CO_2 laser production of fused silica fibers for use in interferometric gravitational wave detector mirror suspensions. *Rev. Sci. Instrum.* **82** (2011). URL http://scitation.aip.org/content/aip/journal/rsi/82/1/10.1063/1.3532770.

[52] Shapiro, B. N. *et al.* Noise and control decoupling of Advanced LIGO suspensions. *Class. Quantum Grav.* **32**, 015004 (2015). URL http://stacks.iop.org/0264-9381/32/i=1/a=015004.

[53] Matichard, F. *et al.* Advanced LIGO two-stage twelve-axis vibration isolation and positioning platform. part 1: Design and production overview. *Precis. Eng.* **40**, 273 – 286 (2015). URL http://www.sciencedirect.com/science/article/pii/S0141635914001561.

[54] Matichard, F. *et al.* Advanced LIGO two-stage twelve-axis vibration isolation and positioning platform. part 2: Experimental investigation and tests results. *Precis. Eng.* **40**, 287 – 297 (2015). URL http://www.sciencedirect.com/science/article/pii/S0141635914002098.

[55] Matichard, F. *et al.* Seismic isolation of Advanced LIGO: Review of strategy, instrumentation and performance. *Class. Quantum Grav.* **32**, 185003 (2015). URL http://stacks.iop.org/0264-9381/32/i=18/a=185003.

[56] Wen, S. *et al.* Hydraulic external pre-isolator system for LIGO. *Class. Quantum Grav.* **31**, 235001 (2014). URL http://stacks.iop.org/0264-9381/31/i=23/a=235001.

[57] Daw, E. J., Giaime, J. A., Lormand, D., Lubinski, M. & Zweizig, J. Long-term study of the seismic environment at LIGO. *Class. Quantum Grav.* **21**, 2255 (2004). URL http://stacks.iop.org/0264-9381/21/i=9/a=003.

[58] Barsotti, L., Evans, M. & Fritschel, P. Alignment sensing and control in Advanced LIGO. *Class. Quantum Grav.* **27**, 084026 (2010). URL http://stacks.iop.org/0264-9381/27/i=8/a=084026.

[59] Staley, A. *et al.* High precision optical cavity length and width measurements using double modulation. *Opt. Express* **23**, 19417–19431 (2015). URL http://www.opticsexpress.org/abstract.cfm?URI=oe-23-15-19417.

[60] Evans, M. *et al.* Observation of parametric instability in Advanced LIGO. *Phys. Rev. Lett.* **114**, 161102 (2015). URL http://link.aps.org/doi/10.1103/PhysRevLett.114.161102.

[61] Rollins, J. G. Distributed state machine supervision for long-baseline gravitational-wave detectors. *Rev. Sci. Instrum.* **87** (2016). URL `http://scitation.aip.org/content/aip/journal/rsi/87/9/10.1063/1.4961665`.

[62] Phelps, M. H., Gushwa, K. E. & Torrie, C. I. Optical contamination control in the Advanced LIGO ultra-high vacuum system. *Proc. SPIE* **8885**, 88852E (2013). URL `https://doi.org/10.1117/12.2047327`.

[63] Smith, M. R. *Scattered Light Control in Advanced LIGO* (World Scientific Publishing Company, 2012). URL `http://www.worldscientific.com/doi/abs/10.1142/9789814374552_0312`.

[64] Brooks, A. F. *et al.* Direct measurement of absorption-induced wavefront distortion in high optical power systems. *Appl. Opt.* **48**, 355–364 (2009). URL `http://ao.osa.org/abstract.cfm?URI=ao-48-2-355`.

[65] Lawrence, R., Zucker, M., Fritschel, P., Marfuta, P. & Shoemaker, D. Adaptive thermal compensation of test masses in Advanced LIGO. *Class. Quantum Grav.* **19**, 1803 (2002). URL `http://stacks.iop.org/0264-9381/19/i=7/a=377`.

[66] Heitmann, H. on behalf of the Virgo Collaboration. Status of the Advanced Virgo gravitational wave detector. *Proc. SPIE* **10700**, 1070017 (2018). URL `https://doi.org/10.1117/12.2312572`.

[67] Granata, M. *et al.* Amorphous optical coatings of present gravitational-wave interferometers (2019). Preprint at `https://arxiv.org/abs/1909.03737`.

[68] Amato, A. *et al.* Optical properties of high-quality oxide coating materials used in gravitational-wave advanced detectors. *J. Phys. Mater.* **2**, 035004 (2019).

[69] Bersanetti, D. *et al.* New algorithm for the Guided Lock technique for a high-Finesse optical cavity. *In press, Astroparticle Physics* (2019). Preprint at `https://doi.org/10.1016/j.astropartphys.2019.102405`.

[70] Acernese, F. *et al.* (Virgo Collaboration). The Advanced Virgo longitudinal control system for the O2 observing run. *Astroparticle Physics, In Press* (2019). URL `https://doi.org/10.1016/j.astropartphys.2019.07.005`.

[71] Aiello, L. *et al.* Thermal compensation system in advanced and third generation gravitational wave interferometric detectors. *J. Phys. Conf. Ser.* **1226**, 012019 (2019).

[72] Cirone, A. *et al.* Investigation of magnetic noise in Advanced Virgo. *Class. Quantum Grav.* **36**, 225004 (2019). Preprint at https://arxiv.org/abs/1908.11174.

[73] Cirone, A. *et al.* Magnetic coupling to the Advanced Virgo payloads and its impact on the low frequency sensitivity. *Rev. Sci. Instrum.* **89**, 114501 (2018). URL https://doi.org/10.1063/1.5045397.

[74] Tringali, M. C. *et al.* Seismic array measurements at Virgo's West End Building for the configuration of a Newtonian-noise cancellation system. *Class. Quantum Grav.* (2019). URL http://iopscience.iop.org/10.1088/1361-6382/ab5c43.

[75] van Heijningen, J. V. *et al.* A multistage vibration isolation system for Advanced Virgo suspended optical benches. *Class. Quantum Grav.* **36**, 075007 (2019).

[76] Chen, H.-Y. *et al.* Distance measures in gravitational-wave astrophysics and cosmology (2017). arXiv:1709.08079.

[77] Abbott, B. P. *et al.* (LIGO Scientific Collaboration, Virgo Collaboration). Low-latency Gravitational-wave Alerts for Multimessenger Astronomy during the Second Advanced LIGO and Virgo Observing Run. *ApJ* **875**, 161 (2019).

[78] Abbott, B. P. *et al.* (LIGO Scientific Collaboration, Virgo Collaboration). Search for intermediate mass black hole binaries in the first and second observing runs of the Advanced LIGO and Virgo network. *Phys. Rev. D* **100**, 064064 (2019).

[79] Finn, L. S. & Chernoff, D. F. Observing binary inspiral in gravitational radiation: One interferometer. *Phys. Rev. D* **47**, 2198–2219 (1993). arXiv:gr-qc/9301003.

[80] Bartos, I. *et al.* The Advanced LIGO timing system. *Class. Quantum Grav.* **27**, 084025 (2010). URL http://stacks.iop.org/0264-9381/27/i=8/a=084025.

[81] Goetz, E. & Savage, R. L. Calibration of the LIGO displacement actuators via laser frequency modulation. *Class. Quantum Grav.* **27**, 215001 (2010). URL https://doi.org/10.1088%2F0264-9381%2F27%2F21%2F215001.

[82] Goetz, E. *et al.* Accurate calibration of test mass displacement in the LIGO interferometers. *Class. Quantum Grav.* **27**, 084024 (2010). URL http://stacks.iop.org/0264-9381/27/i=8/a=084024.

[83] Goetz, E. *et al.* Precise calibration of LIGO test mass actuators using photon radiation pressure. *Class. Quantum Grav.* **26**, 245011 (2009). URL http://stacks.iop.org/0264-9381/26/i=24/a=245011.

[84] Abadie, J. *at al.* (LIGO Scientific Collaboration). Calibration of the LIGO gravitational wave detectors in the fifth science run. *Nucl. Instrum. Methods Phys. Res. A* **624**, 223–240 (2010). URL `http://www.sciencedirect.com/science/article/pii/S0168900210017031`.

[85] Accadia, T. *et al.* (Virgo Collaboration). Reconstruction of the gravitational wave signal h(t) during the Virgo science runs and independent validation with a photon calibrator. *Class. Quantum Grav.* **31**, 165013 (2014).

[86] Accadia, T. *et al.* (Virgo Collaboration). Calibration and sensitivity of the virgo detector during its second science run. *Class. Quantum Grav.* **28**, 025005 (2010).

[87] Viets, A. D. *et al.* Reconstructing the calibrated strain signal in the Advanced LIGO detectors. *Class. Quantum Grav.* **35**, 095015 (2018). `arXiv:1710.09973`.

[88] Acernese, F. *et al.* (Virgo Collaboration). Calibration of Advanced Virgo and Reconstruction of the Gravitational Wave Signal $h(t)$ during the Observing Run O2. *Class. Quantum Grav.* **35**, 205004 (2018).

[89] Cahillane, C. *et al.* Calibration uncertainty for Advanced LIGO's first and second observing runs. *Phys. Rev. D* **96**, 102001 (2017). `arXiv:1708.03023`.

[90] Abbott, B. P. *et al.* (LIGO Scientific Collaboration). Calibration of the Advanced LIGO detectors for the discovery of the binary black-hole merger GW150914. *Phys. Rev. D* **95**, 062003 (2017). URL `https://link.aps.org/doi/10.1103/PhysRevD.95.062003`.

[91] LIGO Scientific Collaboration and Virgo Collaboration. LIGO/Virgo Public Alerts User Guide (2018). URL `https://emfollow.docs.ligo.org/userguide/`.

[92] LIGO Scientific Collaboration and Virgo Collaboration. Data release for event GW150914 (2016). URL `https://www.gw-openscience.org/events/GW150914/`.

[93] LIGO Scientific Collaboration and Virgo Collaboration. Data release for event LVT151012 (2016). URL `https://www.gw-openscience.org/events/LVT151012/`.

[94] LIGO Scientific Collaboration and Virgo Collaboration. Data release for event GW151226 (2016). URL `https://www.gw-openscience.org/events/GW151226/`.

[95] LIGO Scientific Collaboration and Virgo Collaboration. Data release for event GW170104 (2017). URL `https://www.gw-openscience.org/events/GW170104/`.

[96] LIGO Scientific Collaboration and Virgo Collaboration. Data release for event GW170608 (2017). URL `https://www.gw-openscience.org/events/GW170608/`.

[97] LIGO Scientific Collaboration and Virgo Collaboration. Data release for event GW170814 (2017). URL `https://www.gw-openscience.org/events/GW170814/`.

[98] LIGO Scientific Collaboration and Virgo Collaboration. Data release for event GW170817 (2017). URL `https://www.gw-openscience.org/events/GW170817/`.

[99] Martynov, D. V. *et al.* Sensitivity of the Advanced LIGO detectors at the beginning of gravitational wave astronomy. *Phys. Rev. D* **93**, 112004 (2016). URL `https://link.aps.org/doi/10.1103/PhysRevD.93.112004`.

[100] Abbott, B. P. *et al.* (LIGO Scientific Collaboration, Virgo Collaboration). A guide to LIGO-Virgo detector noise and extraction of transient gravitational-wave signals (2019). Preprint at `https://arxiv.org/abs/1908.11170`.

[101] Adhikari, R. *Sensitivity and Noise Analysis of 4 km Laser Interferometric Gravitational Wave Antennae*. Ph.D. thesis, Massachusetts Institute of Technology (2004).

[102] Covas, P. B. *et al.* Identification and mitigation of narrow spectral artifacts that degrade searches for persistent gravitational waves in the first two observing runs of Advanced LIGO. *Phys. Rev. D* **97**, 082002 (2018). `arXiv:1801.07204`.

[103] Fiori, I. O2 lines summary (2017). URL `https://logbook.virgo-gw.eu/virgo/?r=40306`.

[104] Effler, A. *et al.* Environmental Influences on the LIGO Gravitational Wave Detectors during the 6th Science Run. *Class. Quantum Grav.* **32**, 035017 (2015).

[105] Abbott, B. P. *et al.* (LIGO Scientific Collaboration, Virgo Collaboration). Characterization of transient noise in Advanced LIGO relevant to gravitational wave signal GW150914. *Class. Quantum Grav.* **33**, 134001 (2016). `arXiv:1602.03844`.

[106] Abbott, B. P. *et al.* (LIGO Scientific Collaboration, Virgo Collaboration). Effects of Data Quality Vetoes on a Search for Compact Binary Coalescences in Advanced LIGO's First Observing Run. *Class. Quantum Grav.* **35**, 065010 (2018). `arXiv:1710.02185`.

[107] Davis, D. *et al.* Improving the Sensitivity of Advanced LIGO using noise subtraction. *Class. Quantum Grav.* **36**, 055011 (2019). `arXiv:1809.05348`.

[108] Pankow, C. *et al.* Mitigation of the instrumental noise transient in gravitational-wave data surrounding GW170817. *Phys. Rev. D* **98**, 084016 (2018). URL `https://link.aps.org/doi/10.1103/PhysRevD.98.084016`.

[109] Biwer, C. *et al.* Validating gravitational-wave detections: The Advanced LIGO hardware injection system. *Phys. Rev. D* **95**, 062002 (2017). `arXiv:1612.07864`.

[110] Ellis, G. *Control System Design Guide (Fourth Edition)* (Butterworth-Heinemann, 2012).

[111] Jones, E. *et al.* SciPy: Open source scientific tools for Python (2001). URL `http://www.scipy.org/`.

[112] Nyquist, H. Certain factors affecting telegraph speed. *Bell System Technical Journal* **3**, 324–346 (1924).

[113] Nyquist, H. Certain topics in telegraph transmission theory. *Transactions A.I.E.E.* **47**, 617–644 (1928).

[114] Shannon, C. E. Communication in the presence of noise. *Proceedings of the IRE* **37**, 10–21 (1949).

[115] Koziol, Q. & Robinson, D. HDF5 (2018). URL `https://doi.org/10.11578/dc.20180330.1`.

[116] LIGO Scientific Collaboration and Virgo Collaboration. Specification of a common data frame format for interferometric gravitational wave detectors. Tech. Rep. VIR-067A-08 (2009). URL `https://dcc.ligo.org/LIGO-T970130/public`.

[117] Nitz, A. H. *et al.* PyCBC Software. *GitHub repository* (2017). URL `https://github.com/ligo-cbc/pycbc`.

[118] Usman, S. A. *et al.* The PyCBC search for gravitational waves from compact binary coalescence. *Class. Quant. Grav.* **33**, 215004 (2016). `arXiv:1508.02357`.

[119] Sachdev, S. *et al.* The GstLAL Search Analysis Methods for Compact Binary Mergers in Advanced LIGO's Second and Advanced Virgo's First Observing Runs. *submitted to Phys. Rev. D* (2019). Preprint at `https://arxiv.org/abs/1901.08580`.

[120] Cody, M. *et al.* Analysis Framework for the Prompt Discovery of Compact Binary Mergers in Gravitational-wave Data. *Phys. Rev. D* **95**, 042001 (2017). `arXiv:1604.04324`.

[121] Abbott, B. P. *et al.* (LIGO Scientific Collaboration, Virgo Collaboration). Search for Subsolar Mass Ultracompact Binaries in Advanced LIGO's Second Observing Run. *Phys. Rev. Lett.* **123**, 161102 (2019).

[122] Klimenko, S. *et al.* Method for detection and reconstruction of gravitational wave transients with networks of advanced detectors. *Phys. Rev. D* **93**, 042004 (2016). `arXiv:1511.05999`.

[123] Abbott, B. P. *et al.* (LIGO Scientific Collaboration, Virgo Collaboration). All-sky search for short gravitational-wave bursts in the second Advanced LIGO and Advanced Virgo run. *Phys. Rev. D* **100**, 024017 (2019).

[124] Abbott, B. P. *et al.* (LIGO Scientific Collaboration, Virgo Collaboration). An Optically Targeted Search for Gravitational Waves emitted by Core-Collapse Supernovae during the First and Second Observing Runs of Advanced LIGO and Advanced Virgo (2019). Preprint at `https://arxiv.org/abs/1908.03584`.

[125] Lynch, R., Vitale, S., Essick, R., Katsavounidis, E. & Robinet, F. Information-theoretic approach to the gravitational-wave burst detection problem. *Phys. Rev. D* **95**, 104046 (2017).

[126] Littenberg, T. B., Kanner, J. B., Cornish, N. J. & Millhouse, M. Enabling high confidence detections of gravitational-wave bursts. *Phys. Rev. D* **94**, 044050 (2016).

[127] Abbott, B. P. *et al.* (LIGO Scientific Collaboration, Virgo Collaboration). All-sky search for continuous gravitational waves from isolated neutron stars using Advanced LIGO O2 data. *Phys. Rev. D* **100**, 061101 (2019). URL `https://link.aps.org/doi/10.1103/PhysRevD.100.024004`.

[128] Abbott, B. P. *et al.* (LIGO Scientific Collaboration, Virgo Collaboration). Narrow-band search for gravitational waves from known pulsars using the second LIGO observing run. *Phys. Rev. D* **99**, 122002 (2019). URL `https://link.aps.org/doi/10.1103/PhysRevD.99.122002`.

[129] Abbott, B. P. *et al.* (LIGO Scientific Collaboration, Virgo Collaboration). Searches for Gravitational Waves from Known Pulsars at Two Harmonics in 2015–2017 LIGO Data. *ApJ* **879**, 10 (2019).

[130] Search for gravitational waves from Scorpius X-1 in the first Advanced LIGO observing run with a hidden Markov model. *Phys. Rev. D* **95**, 122003 (2017).

[131] Abbott, B. P. *et al.* (LIGO Scientific Collaboration, Virgo Collaboration). Upper limits on the stochastic gravitational-wave background from Advanced LIGO's First Observing Run. *Phys. Rev. Lett.* **118**, 121101 (2017). URL `https://link.aps.org/doi/10.1103/PhysRevLett.118.121101`.

[132] Abbott, B. P. *et al.* (LIGO Scientific Collaboration, Virgo Collaboration). Search for the isotropic stochastic background using data from Advanced LIGO's second observing run. *Phys. Rev. D* **100**, 061101 (2019). URL https://link.aps.org/doi/10.1103/PhysRevD.100.061101.

[133] LIGO Scientific Collaboration and Virgo Collaboration. H1 lines cleaning file for O1 - version 3 (2015). URL https://www.gw-openscience.org/static/speclines/o1/O1LinesToBeCleaned_H1_v3.txt.

[134] LIGO Scientific Collaboration and Virgo Collaboration. L1 lines cleaning file for O1 - version 3 (2015). URL https://www.gw-openscience.org/static/speclines/o1/O1LinesToBeCleaned_L1_v3.txt.

[135] LIGO Scientific Collaboration and Virgo Collaboration. H1 lines cleaning file for O2 - version 2 (2019). URL https://www.gw-openscience.org/static/speclines/o2/O2LinesToBeCleaned_H1_v2.txt.

[136] LIGO Scientific Collaboration and Virgo Collaboration. L1 lines cleaning file for O2 - version 2 (2019). URL https://www.gw-openscience.org/static/speclines/o2/O2LinesToBeCleaned_L1_v2.txt.

[137] LIGO Scientific Collaboration and Virgo Collaboration. List of lines for Virgo V1 during O2 - 20190209, version 1 (2019). URL https://www.gw-openscience.org/static/speclines/o2/O2_lines_Virgo_V1.txt.

[138] LIGO Scientific Collaboration and Virgo Collaboration. Data quality vetoes applied to the analysis of GW150914. hhttps://dcc.ligo.org/public/0123/T1600011/003/DQdoc.pdf (2016).

[139] Gravitational Wave Open Data Workshop Web Courses, 2018 and 2019. https://www.gw-openscience.org/tutorials/.

[140] Kluyver, T. *et al.* Jupyter notebooks – a publishing format for reproducible computational workflows. In *Positioning and Power in Academic Publishing: Players, Agents and Agendas*, 87 – 90 (IOS Press, 2016).

[141] LIGO Scientific Collaboration. Source code for: LIGO Algorithm Library - LALSuite (2018). https://doi.org/10.7935/GT1W-FZ16.

[142] Macleod, D. *et al.* Source code for: GWpy software (2019). https://doi.org/10.5281/zenodo.2603187.

[143] Home page for: GstLAL – https://wiki.ligo.org/Computing/DASWG/GstLAL.

[144] Ashton, G. *et al.* BILBY: A User-friendly Bayesian Inference Library for Gravitational-wave Astronomy. *The Astrophysical Journal Supplement Series* **241**, 27 (2019). DOI of the code: 10.5281/zenodo.2602178.

[145] Veitch, J. *et al.* Parameter estimation for compact binaries with ground-based gravitational-wave observations using the LALInference software library. *Phys. Rev. D* **91**, 042003 (2015).

[146] Cornish, N. J. & Littenberg, T. B. Bayeswave: Bayesian inference for gravitational wave bursts and instrument glitches. *Class. Quantum Grav.* **32**, 135012 (2015). arXiv:1410.3835.

[147] Littenberg, T. B. & Cornish, N. J. Bayesian inference for spectral estimation of gravitational wave detector noise. *Phys. Rev. D* **91**, 084034 (2015).

[148] Gravitational wave open science center (GWOSC). http://www.gw-openscience.org.

[149] GWTC-1: A Gravitational-Wave Transient Catalog of Compact Binary Mergers Observed by LIGO and Virgo during the First and Second Observing Runs (2018). URL https://dcc.ligo.org/LIGO-P1800307/public. DOI https://doi.org/10.7935/82H3-HH23.

[150] How to acknowledge use of LIGO/Virgo data through GWOSC. https://www.gw-openscience.org/acknowledgement/.